The Hydrodynamics of Sailboat Bailing Devices

by

Britton Reynolds Ward

B.S. Naval Architecture and Marine Engineering (1995)
Webb Institute of Naval Architecture

Submitted to the Department of Ocean Engineering
in Partial Fulfillment of the Requirements for the Degree of

Master of Science in Ocean Engineering

at the

Massachusetts Institute of Technology

September, 1996

Signature of Author .....
Department of Ocean Engineering
July 31, 1996

Certified by .....
Jerome Milgram
Professor of Ocean Engineering
Thesis Supervisor

Accepted by .....
A. Douglas Carmichael
Chairman, Department Committee on Graduate Students

The Hydrodynamics of Sailboat Bailing Devices

by

Britton Reynolds Ward

Submitted to the Department of Ocean Engineering in Partial Fulfillment of
the Requirements for the Degree of Master of Science in Ocean Engineering.

Abstract

This paper outlines the design and construction of an experiment to establish the relative performance characteristics of sailboat bailing devices. Data was obtained for a series of production bailers, newly designed prototypes and production bailer variations allowing classification of their relative performance with regard to flow rate, minimum speed of bailing inception and drag. These results were non-dimensionalized and this information used to examine the effects of bailer geometry on performance in these critical categories.

The experimental data conclusively show that a prototype developed from the current generation of production bailers produces in excess of three times the flow rate of the parent production bailer and is capable of operation at a significantly lower speeds. This bailer has an acceptable increase in measured drag over the production bailer baseline. A theory is advanced as to the reasons for these dramatic improvements in performance and this corroborated with visual observations of the bailer in operation.

A study of operational considerations is also incorporated and these observations used in defining design requirements for a production version of the best prototype. A proposed production design is outlined incorporating these suggested operational requirements.

Thesis Supervisor: Dr. Jerome Milgram
Title: Professor of Ocean Engineering

Acknowledgements

Many people contributed to the preparation of this thesis and without their help and support the incredible success of the project would not have been possible. I am greatly indebted to Professors Jerome Milgram and Douglas Carmichael for their continued patience, instruction and support throughout the course of this project. Their guidance and suggestions always provided a way to turn when all seemed questionable.

To the students of the Independent Activities Program Course "Design a Better Bailer" I am thankful for your enthusiasm, ideas and assistance in the initial planning stages of the experiment and your continued help throughout the semester in completing the testing program. Recognition is also due to Richard Kimball and the students of the Marine Hydrodynamics Laboratory for their assistance in running experiments and finding the time to allow me to complete the experimental program.

Without the financial assistance and initial motivation of Mr. William Shore and Mr. Peter McCarthy of U.S. Sailing and the United States Olympic Committee this project would not have been possible. Further financial support from the America^3 Foundation, Mr. Matthew Tobriner and Mr. Karl Kirkman of Science Applications International Corporation was essential to the completion of the project and I am grateful for their assistance. Mr. Tobriner's continued interest in the project and his willingness to help in every way are greatly appreciated. I am grateful for Mr. Arnold Heitmann's interest and his inventiveness that was so essential in the development of operationally effective prototype bailers at the hectic conclusion of this project.

I would especially like to thank: Jaye Falls for sticking with me through a tough and trying year; My parents, Richard and Gayle, brothers Tyler and Harrison and sisters Whitney and Teagan, who all have been an incredible source of encouragement and support for me over the years - even from 12,000 miles away in Australia.

Table of contents

List of Illustrations and Figures

List of Tables

List of Symbols

A	Reservoir Test Section Area. [m^2, ft^2]
A_{proj}	Bailer Projected Area, [m^2, ft^2]
C_p	Non-Dimensional Pressure Coefficient
C_d	Non-Dimensional Drag Coefficient
c	Foil Section Chord Length
x	Foil Section Chordwise Position, Boundary Layer Development Length
P_1, P_2, P_3, P	Pressures, Subscript Denotes Location, [Pa, psi]
ΔP	Pressure Difference, [Pa, psi]
Q	Volumetric Flow Rate, [m^3/s, ft^3/s]
Re	Reynolds Number = UL/ν
u	Perturbed Velocity, [m/s, ft/s, knots]
U	Free Stream Velocity, [m/s, ft/s, knots]
V, V_1, V_2, V_3	Fluid Velocity, Subscript Denotes Location, [m/s, ft/s, knots]
δ	Boundary Layer Thickness, [mm]
ν	Kinematic Viscosity of Water, [m^2/s]
ρ	Density of Water, [kg/m^3, $slug/ft^3$]

Chapter 1 - Introduction

Since the advent of popularized yacht racing almost every means of maintaining a speed advantage over the competition has been explored. One of the greatest contributors to resistance and therefore loss of speed occurs when the yacht is sailed at a draft greater than the design draft. Should an increase in draft occur the wetted surface area of the hull will increase and greater frictional and residuary resistance will result. Such an increase in displacement is the result of the shipping of water into the hull, whether through large angles of heel (potentially from capsizing) or through the advent of spray caused by the boat's motion through a seaway. By keeping the cockpit or bilge dry the crew can be sure to maintain the yacht at its design draft thus minimizing the additional resistance. Of course it's next to impossible to prevent the shipping of spray, and removing this water efficiently can be of great benefit in maintaining the yacht at its optimum sailing trim.

Methods of removing this water efficiently include both powered and mechanical pumping mechanisms which in most cases are only suitable for larger craft. In light of this, the last thirty years have seen the development of a number of self bailing devices that utilize the hydrodynamics of flow around the hull to create suction and draw this water out of the hull. Many of the devices currently in use stem from the original bailers developed thirty years ago and are largely a product of manufacturing simplicity and operational considerations rather than development of optimized designs based on the actual hydrodynamics of the flow around the hull and the bailer itself. This thesis presents an experimental analysis of a wide range of production and proposed bailers on the basis of flow rate, minimum bailing speed and drag while deployed, in an effort to isolate those

factors which contribute to improved bailer performance. A baseline production bailer was also taken and modified to isolate the effects of side walls and outflow hole size. Finally the flow rate, minimum operating speed and drag characteristics were synthesized to produce a prototype bailer achieving marked improvements over the current generation of production bailers. A set of systematic experiments was completed to identify those factors significantly affecting the hydrodynamic performance of different bailer designs and these observations used in the development of the final prototype design.

Chapter 2 - Background

2.1- Bailer Application

Many sailboats ranging from racing dinghies to small cruisers utilize small self bailing devices located along the hull to draw water out of the vessel without requiring manual or motorized pumping mechanisms. These bailers perturb the yacht's pressure field and when a certain minimum speed is reached, a low pressure or suction region is created behind the bailer drawing out the water located in the bilge or cockpit. These bailers are usually positioned near midships and consist principally of a small trap door (the face) that closes flush with the skin of the hull so as to minimize drag when not in operation. Attached to the face plate is a closed channel with a small trap door on the down stream end which is free to pivot when outflow occurs but will close and seal the bailer when backflow begins. The bailers are operated by disengaging the locking mechanism and pushing the bailer down manually, reapplying the locking mechanism causes the plate and channel to be withdrawn into the boat and a seal to be created with the top of the face plate, the outer channel wall and a soft rubber compound located within the housing of the bailer. This sealing method eliminates all but the most minute amount of leakage. The typical bailer geometry is depicted in Figure 2.1.

To date bailers are currently manufactured from stainless steel, using a rubber sealing compound, although currently some bailers, most notably for the Laser class of single-handers, are manufactured using an injected plastic molding technique.

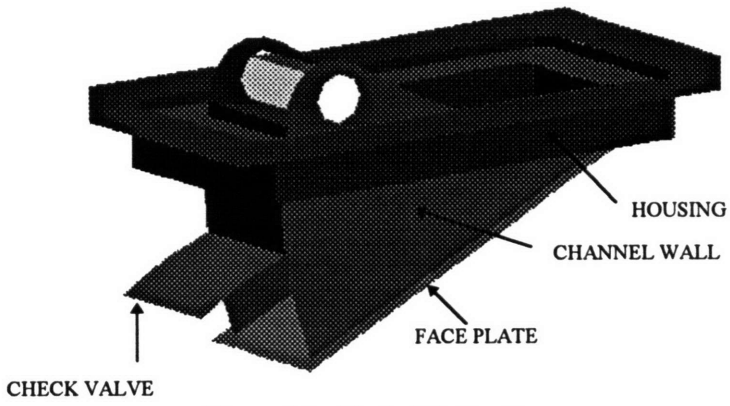

Figure 2.1 - Typical Bailer Geometry

2.2 - Bailer Installation and Vessel Type

As mentioned previously, the self bailing devices of the type depicted in Figure 2.1 are commonly found on racing dinghies with single skin bottoms, larger keel boat racers and in some cases on larger yachts with cockpits susceptible to flooding and lacking manual or motorized pump suction in this area of the vessel. The experimental work developed for this bailer project has principally been concerned with the three Olympic classes where the competitors race their own yachts; the 470, Soling and Star classes. Of course there is a dramatic difference between the 470 and the Soling and Star classes in that the 470 is a planing dinghy while the Star and Soling classes are displacement yachts. For all classes of yacht the hydrodynamics are such that the flow can be utilized to create a suction on the downstream side of the bailer allowing outflow to occur. Of course the magnitude of the flow rate is directly related to the vessel's speed and the geometric configuration of the bailer. Typically larger yachts such as the Soling and Star have been fitted with much larger bailers than the smaller dinghies following the observation that these larger yachts have a greater interior volume and can thus ship much more water. In fact, in the case of the Star class, many of the yachts have opted for manual pumping

mechanisms that can be operated remotely using lanyards from the hiked out position. While the skin mounted self bailing device may be more efficient the disruption in sailing required to open and close it is seen as a severe practical liability. This emphasizes the importance of practical and operational considerations in the development of a successful design.

Practical rather than hydrodynamic considerations also seem to have governed the positioning of the bailers on particular craft. For instance, the 470 class of planing dinghies is limited to two bailers. Customarily one is placed adjacent to the centerboard trunk so as to protect both bailer and crew from damage, while the other is placed on the opposite side somewhat aft. The forward bailer is positioned close to the lowest point of the cockpit so as to provide the largest static head in the level trim sailing condition, while the aft bailer is operated by the skipper, usually in the planing mode when the boat is trimmed aft and the crew is sailing on the trapeze wire. These bailers are both smaller than those fitted to the larger yachts reflecting both practical considerations and the limitations on effective bailer area posed by the class rules. As a transomed planing dinghy the 470's are also fitted with stern flaps that can be opened in the planing condition to allow water to run off into the wake taking advantage of the boat's bow up attitude to allow for bailing without a drag penalty. Like the 470's, both the Star and Soling classes have bailer locations determined largely through practical and operational considerations. Recent trends in these classes is to orient the bailers, not near the center line at the region of greatest hull depth, but closer to the turn of the bilge or even on the side skin above the chine in the Star boat class. In this case the bailers are oriented not fore and aft but

generally in line with the pressure wave created by the hull. By orienting the bailer with the pressure wave it is felt that the flow passing over the bailer is accelerated, thus improving the bailing rate of the deployed bailer. By mounting the bailers further up on the side shell, the static head of water above the bailer is reduced at level heel, however, the keelboats are often not sailed at a level heel and thus the leeward bailer will work successfully provided the water level remains above the bailer inlet. Exploration of the importance of bailer position on the hull to achieve the greatest velocity across the bailer and studies of the effect of bailer skew away from the mean stream angle have not been investigated, due to limitations with testing apparatus and time constraints.

2.3 - Importance of Bailer Optimization

Independent of the bailer position and orientation on the hull there is a great deal of study required to understand the hydrodynamic factors affecting bailer performance. The current generation of bailer designs as outlined above appear to be manufactured largely through consideration of practical design considerations. For instance the use of the channel welded to the larger face plate presents a hard angle that when combined with the rubber sealing in the housing minimizes leakage in the retracted condition. Similarly the check valve door uses a simple pin type hinge, and restricts the potential outflow area to, in some cases, less than half of the available area on the downstream end of the channel. Of course this reduction in area improves the structural rigidity of the channel but it is certain this restriction adversely affects the achievable flow rate of the bailer.

Similarly, examination of a family of bailers indicates a somewhat random selection of dimensions, whether in width of the flange, depth of face protrusion in the operable

mode, width of the channel or length of the whole bailing mechanism. While all production bailers considered have the same general arrangement, this variance in bailer dimensions does present the question which bailer bails the best and why? Can an optimum bailer be designed taking into account all of these various parameters, and taking the best advantage of the hydrodynamics of the flow?

But what defines an optimum choice of bailer? The ideal bailer would have the greatest flow rate, lowest drag when deployed, be able to operate at the lowest possible speed, be largely self operated, prevent any back flow and would seal completely when closed. Such a bailer would clearly be the best in all considerations but it is doubtful that such a bailer can be created. Instead, a compromise design needs to be reached that incorporates features producing the best overall performance, albeit a tradeoff from the best performance in any one area alone. To approach this problem a large variety of bailers with different geometric configurations were tested to characterize their flow rate, minimum bailing speed and drag. Once these characteristics were determined, comparison of each category permitted the isolation of those features that contribute to greater efficiency and lead to the selection of a design that has the best overall performance.

Of course the ideal drag due to a bailer is zero, and while the drag might be low when bailing is occurring as a result of the addition of flow into the stream from the bailer, drag created when the bailer is not working can be considerable. When considering drag in determining an optimum bailer it is important to compare the drag of the bailer with that of the hull in the sailing condition. This ratio, however, is somewhat misleading because the bailer has three distinct modes of operation; the condition when bailing occurs, the

condition when the bailer is down but speed is insufficient to cause bailing and when suction is sufficient to drain the boat entirely and to proceed to draw out air. This last condition will subsequently be called the "ventilation" condition. These three regimes of operation have respectively greater amounts of drag associated with them and thus any optimum drag condition must consider all three modes of operation. Beyond this it is important to relate the effect of the bailing process to the overall drag of the vessel. The increase in wetted surface due to increased displacement may considerably increase the amount of resistance (the exact magnitude of this increase is dependent on the particular hull form) and thus the true drag penalty from use of the bailer must be compared to the extent to which it reduces overall drag through reduction in displacement. Consideration of these relative drag measurements is explored in Chapter 7.

2.4 - History of Bailer Types

The idea of placing an object into the flow to perturb the pressure field and create a suction to draw water out of the hull has been approached in a number of ways. Although the current geometry of bailers as depicted in Figure 2.1 has remained largely unchanged throughout the last thirty years, this current design was preceded by a configuration consisting principally of a retractable cylinder and a back flooding check valve mechanism. The retractable cylinder has an end plate and a notch removed from the back side near the end plate intersection from which the outflow occurred. On the interior of the boat a perforated housing plate attached to the inner bottom allowed for water to flow into the cylinder and be ejected, however, should the yachts speed be too low, the

back flooding water will force a rubber membrane up sealing the perforated plate. This configuration is depicted in Figure 2.2.

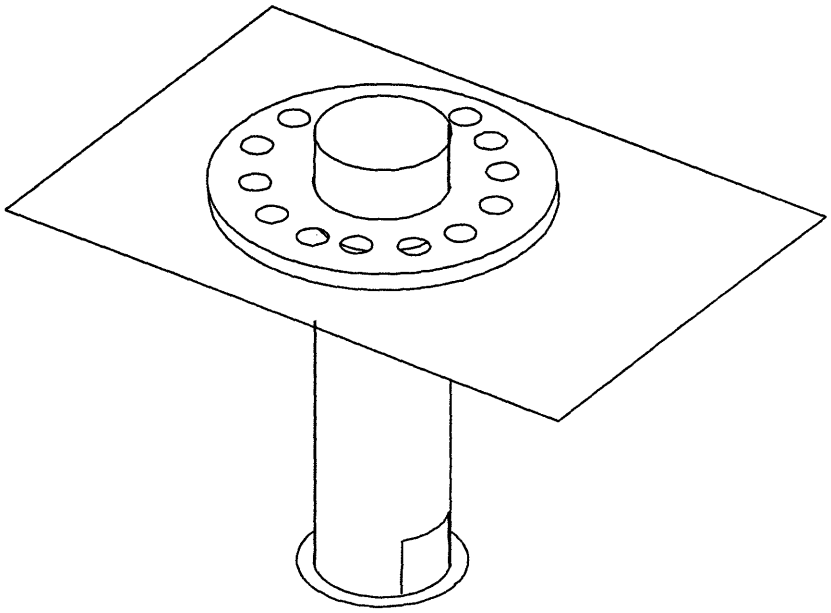

Figure 2.2 - Superseded Cylindrical Bailing Device

While effective, particularly considering the proximity of the outflow notch to flow traveling at the free stream velocity, the choice of a cylindrical section dramatically increases the drag force on the bailer. Operational considerations also limit the value of this bailer considering the possible risk to the crew when the bailer is in the retracted condition. Within the past thirty years bailers of this type have been completely superseded by the more modern Andersen - Elvstrom type of bailers such as those depicted in Figure 2.1. Modifications and developments upon these bailers have largely been to simplify manufacturing rather than to improve performance and it is with this in mind that a more rigorous experimental study of the features of the bailers has been undertaken.

2.5 - General Theory Behind Bailer Hydrodynamics

The principal hydrodynamic principle behind the operation of an Elvstrom type bailer lies in the perturbation of the flow field around the hull and the bailer body. When the flow accelerates around the bailer, it creates a low pressure region immediately behind the trailing face. The region of low pressure or suction draws the water out of the boat until the suction pressure is equal to the hydrostatic pressure of water above the bailer, i.e. equilibrium is reached. Above a certain speed this suction pressure will be below atmospheric pressure and ventilation will occur.

In an attempt to understand the physical nature of the fluid flow around the bailer a simple experiment was conducted. The data obtained from this experiment was used to gain order of magnitude values for the acceleration of the fluid around the bailer and to explore the relationship of pressures in three critical locations; firstly, behind the bailer, secondly, below and forward of the bailer and thirdly above the bailer. These locations can be seen in Figure 2.3.

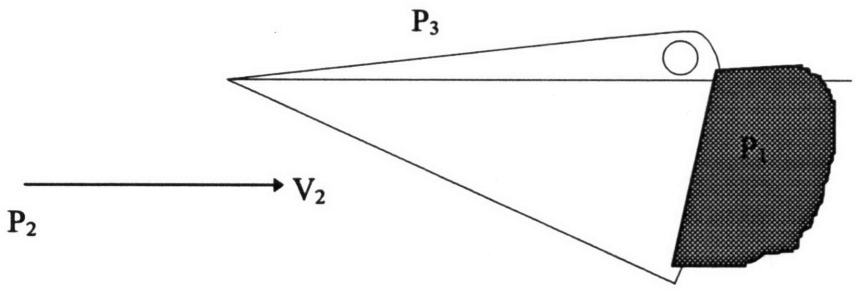

Figure 2.3 - Pressure Locations

The minimum speed required to allow bailing to occur is the speed at which the suction pressure, P_1, and the hydrostatic pressure of the water in the boat, P_3, are equal.

Utilizing this condition, along with Bernoulli's equation applied along a stream line around the bailer, a relation between the change in velocity and pressure due to the bailers perturbation of the flow can be made. Expressing the Bernoulli equation for a stream line passing around the bailer and out of the influence of the wake as:

$$P_1 + \tfrac{1}{2}\rho V_1^2 + gz_1 = P_2 + \tfrac{1}{2}\rho V_2^2 + gz_2 \qquad \text{Equation 2.1}$$

This can be re-written in the following form where the potential energy is eliminated:

$$\tfrac{1}{2}\rho (V_1^2 - V_2^2) = P_2 - P_1 \qquad \text{Equation 2.2}$$

The suction pressure P_1 is difficult to accurately measure, however, in the equilibrium condition $P_1 = P_3$ so that equation 2.2 becomes:

$$\tfrac{1}{2}\rho (V_1^2 - V_2^2) = P_2 - P_3 \qquad \text{Equation 2.3}$$

The pressures P_2 and P_3 can be determined by visual measurement of the head of water using a manometer and by applying the hydrostatic pressure relation $P = \rho gh$. The pressure P_2 represents the dynamic pressure caused by the motion of water past the bailer and can be measured at any point in the fluid below the bailer provided a hydrostatic correction for the difference between the point of pressure measurement and the point at the bailer interface is added. The pressure P_3 represents the total hydrostatic head of water above the bailer interface. Now defining $\Delta P = P_2 - P_3$ and manipulating Equation 2.3 we are left with:

$$\frac{\Delta P}{\frac{1}{2}\rho V_2^2} = \left(\frac{V_1}{V_2}\right)^2 - 1 \qquad \text{Equation 2.4}$$

The left hand side represents the non-dimensional pressure coefficient and can be calculated directly once the head difference between the two desired locations is known

and the free stream speed, V_2, is recorded. A series of four runs was completed using the Super Medium production bailer as an example. The following results were obtained:

Table 2.1 - Bailer Velocity Perturbation Experiment Results

Speed, V ft/sec	ΔHead Reading, ft	$\Delta Head/V^2$, s^2/ft	$\Delta P/(0.5\rho V^2)$
6	0.229	0.0064	0.412
9	0.500	0.0062	0.399
10.2	0.640	0.0062	0.399
11.96	0.875	0.0061	0.394

Examination of the non-dimensional pressure coefficients in the last column indicate that the non dimensional pressure coefficient for this bailer is approximately equal to 0.4. Substituting into Equation 2.4 we note that:

$$V_1/V_2 \approx 1.18$$

Thus indicating that the flow is accelerated some 20% by passing around the bailer. This experiment serves to illustrate the application of Bernoulli's equation along a stream line in relating the pressure and flow velocity around the bailer.

In a similar fashion the preliminary estimates of the expected drag force on a bailer can be made. The drag force on the bailer can initially be assumed to be the combined effects of pressure drag behind the projected area of the bailer and frictional drag components over the channel side plates. This assumes that the pressure drag over the bailer face plate is negligible. Considering a Super Max production bailer fitted to a Star class yacht, traveling at 10 feet per second an initial estimate of the bailer drag and how this drag compares to the yacht's drag can be completed.

Consider the pressure drag generated over the projected area of the deployed bailer:

Boat Velocity, U = 10 ft/s (3.048 m/s, 5.924 knots)
Density of Water, $\rho = 1000\ kg/m^3$
Super Max Bailer Projected Area, $A_{proj} = 0.00147\ m^2$
Bailer Pressure Coefficient, $C_p = \Delta P/\frac{1}{2}\rho U^2 = 0.4$ (Determined Previously)

Pressure Drag, $D_p = \frac{1}{2}C_p\rho U^2 A_{proj} = \frac{1}{2}(0.4)(1000)(3.048)^2(0.00147)$
$D_p = 2.73\ N\ (0.61\ lbf)$

Now consider frictional drag over the channel side wall surface:

Assuming a frictional drag coefficient, $C_f = 0.005$
Super Max Bailer Sidewall Area (Both Sides), $A_s = 0.00318\ m^2$

Frictional Drag, $D_f = \frac{1}{2}C_f\rho U^2 A_s = \frac{1}{2}(0.005)(1000)(3.048)^2(0.00318)$
$D_f = 0.074\ N\ (0.017\ lbf)$

So the total bailer drag is the sum of the frictional and pressure drag values:

Total Bailer Drag, $D_{tb} = D_p + D_f = 2.80\ N\ (0.63\ lbf)$

The drag on the Star boat travelling at 10 feet per second in a level heel attitude can be obtained from velocity prediction program output and tank test results as furnished by U.S. Sailing.

Waterline Length, LWL (As used in Velocity Prediction Program) = 17.825 ft
Yacht Speed, V = 10 ft/s = 5.924 knots
Speed to Length Ratio = V(knots)/(LWL(ft))^0.5 = 1.40

Total Boat Resistance = 253.61 N (56.99 lbf)
so, the estimated drag of the bailer is 1.1% of a Star yacht's resistance at 10 ft/s.

One percent is a significant proportion of the yacht's drag and serves to emphasize the importance of improved bailer performance, whether through a reduction in the time of deployment by improving flow rate, or through designing a bailer with reduced drag in operation. Further consideration of the bailer drag is discussed in Chapter 7.

Chapter 3 - Design of an Experimental Method to Characterize Bailer Performance

3.1 - Critical Parameters Determining Bailer Performance

Methods of characterizing bailer performance must be addressed before a complete experiment can be devised which determines the relative merits and weaknesses of any individual bailer. As outlined before, the critical parameters that reflect a bailer's performance are:

- Bailer volumetric flow rate
- Minimum operating speed
- Bailer drag in the various modes of operation

As defined in Section 2.5 the minimum bailing speed occurs when the suction and hydrostatic pressure acting externally on the bailer at a particular speed is equal to the internal hydrostatic pressure above the bailer. When the suction pressure is lower than the hydrostatic pressure in the boat, outflow will occur. As a result, the pressure difference at equilibrium is the minimum operating ΔP. Noting that the suction created at the bailer trailing face is solely a function of dynamic pressure and equating this to the hydrostatic pressure difference acting on the bailer the minimum speed of bailing inception can be determined.

Perhaps the most important parameter representing the capabilities of a bailer is the volumetric flow rate. For an experiment to evaluate bailer performance, if the bailer is supplied by a reservoir of constant cross section the volumetric flow rate, Q, of outflow through the bailer, can be directly related to the rate of change of the height of the water

level in the reservoir and to the pressure above the bailer interface using the following relations:

$$Q = -\frac{dV}{dt} = -\frac{d}{dt}Ah = -A\frac{dh}{dt} = -\frac{A}{\rho g}\frac{dP}{dt} \qquad \text{Equation 3.1}$$

Where,

Q = *Volumetric Flow Rate,* m^3/s
V = *Outflow Volume,* m^3
A = *Reservoir Cross Sectional Area,* m^2
h = *Height of Water in the Reservoir, m*
ρ = *Density of Water,* kg/m^3
P = *Hydrostatic Pressure Above Bailer, Pa* (N/m^2)
g = *Acceleration Due to Gravity,* m/s^2

The volumetric flow rate of the bailer is represented by the change in hydrostatic pressure above the bailer interface with time. Measurement of the pressure at the external interface of the bailer is important in establishing the speed of bailing inception. In the experiments the external pressure on the bailer increases over time, due to the added water volume expelled from the reservoir going into the tunnel. This effect is eliminated in the reduced data by relating the flow rate to the change in pressure difference over time so that a true measure of the bailers flow rate and minimum operating pressure difference can be achieved.

Numerous methods are available for the determination of the drag on a particular bailer. These may include use of Laser Doppler Velocimetry (LDV) to map the velocity field from which the momentum equation can be solved and the drag force on the body determined. Such a method was, however, precluded due to the arrangement of the

experimental apparatus. A much simpler method incorporates the use of a load cell which outputs a variable voltage dependent on the size of the load encountered. Details of the incorporation of this method into the experiment and of the problems that were encountered are considered subsequently.

3.2 - Non-Dimensionalization of Governing Parameters

To allow for comparison between the variety of prototypes considered, the critical parameters governing bailer performance must be non-dimensionalized. We can consider our three essential parameters as functions of a number of independent parameters represented as follows:

$$Drag,\ D = f_1(U, L, \rho, \mu, \delta, P_3 - P_2)$$

$$Flow\ rate,\ Q = f_2(U, L, \rho, \mu, \delta, P_3 - P_2)$$

$$Minimum\ Bailing\ Speed,\ U_{min} = f_3(U, L, \rho, \mu, \delta, P_3 - P_2)$$

Arranging the variables of functions 1 through 3 into non-dimensional groups and expressing the desired parameters in non-dimensional form we see that the above functional relationships can be expressed as:

$$Drag:\ f_1'(\rho UL/\mu,\ \Delta P/(\tfrac{1}{2}\rho U^2),\ \delta/L) = D/(\tfrac{1}{2}\rho U^2 L^2)$$

$$Flow\ rate:\ f_2'(\rho UL/\mu,\ \Delta P/(\tfrac{1}{2}\rho U^2),\ \delta/L) = Q/UL^2$$

$$Minimum\ Bailing\ Speed:\ f_3'(\rho UL/\mu,\ \Delta P/(\tfrac{1}{2}\rho U^2),\ \delta/L) = U_{min}/U$$

Where,

ρ = *mass density of water,* kg/m^3
P_3 = *Reservoir Pressure on Bailer Interface, Pa*
P_2 = *External Pressure on Bailer Interface, Pa*

$\Delta P = P_3 - P_2$ = *Pressure Differential Across Bailer Interface, Pa*

L = *Designated Length Scale, m*

μ = *Dynamic Viscosity Term, kg/m-sec*

U = *Free Stream Velocity, m/s*

δ = *Boundary Layer Thickness, m*

Observe that for a constant speed, the Reynolds number term, $Re = \rho UL/\mu$, will remain constant and can thus be removed from the functional dependencies expressed above. The third independent parameter is the non-dimensional boundary layer thickness, δ/L which is directly related to Reynolds number via the 1/7th velocity power law approximation for the turbulent boundary layer thickness over a flat plate [3]:

$$\delta = 0.373 \times Re^{-1/5} \qquad \text{Equation 3.2}$$

δ is dependent on both the boat type and its speed of travel and a detailed study of boundary layer effects on the flow rate performance of the bailer would considerably increase the complexity of the experiment. The tests did not vary boundary layer thickness although estimates of the boat boundary layer thicknesses compare can be compared to those measured in the propeller tunnel as can be seen in Table 3.1.

Drag: $f_1''(\Delta P/(\frac{1}{2}\rho U^2)) = D/(\frac{1}{2}\rho U^2 L^2)$

Flow rate: $f_2''(\Delta P/(\frac{1}{2}\rho U^2)) = Q/UL^2$

Minimum Bailing Speed: $f_3''(\Delta P/(\frac{1}{2}\rho U^2)) = U_{min}/U$

This indicates that the primary non-dimensional variable affecting all physical phenomena is the pressure coefficient, $C_p = \Delta P/(\frac{1}{2}\rho U^2)$, where ΔP is the differential pressure across the bailer interface.

It has already been established that both the bailing inception speed and the flow rate can be determined through measurement of the pressures at the bailer interface. Similarly, raw drag results can be determined through the use of a load cell provided the experimental apparatus is suitably designed. The pressure coefficient can be easily determined using the known free stream velocity and the density of water. Similarly, the flow rate and drag can be non-dimensionalized once a length scale is chosen. Both flow rate and drag are non-dimensionalized with respect to L^2 and hence an area is most appropriate for use as the squared length scale term. In determining which area should be adopted it is important to recognize that the chosen area must have physical relevance to the parameter at hand. In the determination of drag it is apparent that both pressure and frictional drag components are at work and consequently both the total wetted area of the bailer and the projected area that generates the suction are relevant. Further complicating this decision, a number of different areas, all of which would be suitable for non-dimensionalizing flow rate, are available. These include the projected area which is related to the generation of suction, the outflow hole area that limits the flow rate and the total outflow channel area that acts also as a measure of the depth of the bailer away from the hull. All of these areas are relevant and have physical significance; however, to allow for comparison, it is useful to use the same area for both drag and flow rate non-dimensionalizations. Accordingly, it was decided to adopt the downstream projected area of the bailer as the L^2 parameter. This area incorporates the effect of the larger face plate and acknowledges that the size of this area is directly related to the magnitude of the suction produced. Further supporting this choice is the fact that the pressure drag

produced in this region is much larger in magnitude than the frictional drag component which is related to the total wetted surface area of the bailer.

If it is assumed that the bailer flow rate is solely a function of acceleration due to the change in pressure across the bailer outlet, commonly referred to as orifice flow, then a functional form relating the flow rate and the measured pressures and velocities can be derived.

Using the nomenclature defined in Figure 2.3,

if $\Delta P_1 = P_3 - P_1$ where, P_1 is the suction pressure and P_3 is the reservoir pressure and

$\Delta P = P_3 - P_2$ where P_2 is the external bailer pressure then;

assuming orifice flow such that: $\Delta P \propto \rho U^2$

then, $$\Delta P_1 = \Delta P + c'\rho U^2 \qquad \text{Equation 3.3}$$

since $P_2 - P_1 = c'\rho U^2$ where c' is a constant. The outflow velocity, u, can thus be expressed as:

$$u = m'\sqrt{\frac{\Delta P_1}{\rho}} \qquad \text{Equation 3.4}$$

but $u = Q/A$, so substituting Equation 3.3 into Equation 3.4,

$$\frac{Q}{A} = m'\sqrt{\frac{\Delta P + c'\rho U^2}{\rho}} \qquad \text{Equation 3.5}$$

Dividing both sides by U:

$$\frac{Q}{UA} = m'\sqrt{c' + \frac{\Delta P}{\rho U^2}} \qquad \text{Equation 3.6}$$

Manipulating, we are left with the following relationship:

$$\left(\frac{Q}{UA}\right)^2 = m\frac{\Delta P}{\rho U^2} + c \qquad \text{Equation 3.7}$$

Where,

Q = *Volumetric Flowrate,* m^3/s

U = *Free Stream Velocity, m/s*

A = *Projected Outflow Area,* m^2

ρ = *Mass Density of Water,* kg/m^3

ΔP, ΔP_1, P_1, P_2, P_3 = *Pressures as defined above, Pa*

m, m', c, c' = *Constants*

Provided the assumptions of orifice flow and neglible boundary layer effects are correct, a linear relationship should hold between non-dimensional flow rate squared and the pressure difference across the bailer.

3.3 - Apparatus Design

Having established the required parameters for testing, the design of the experimental apparatus was undertaken to ensure experimental repeatability and that an accurate means of obtaining both pressure and drag data was available. The bailer experimental apparatus was designed to utilize the features of the Variable Pressure Water Tunnel Located in the Marine Hydrodynamics Laboratory of the Massachusetts Institute of Technology. A general schematic of the water tunnel is shown in Figure 3.1, and highlights the position of the test section, impeller location, tunnel contractions and expansions and the location of the fill pot downstream of the test section. The test section is surrounded on all four sides by two inch thick plexi-glass windows that are easily removed and present an ideal foundation for the basis of the experiment.

For an accurate relation between the experimental test of a bailer and its real operating condition, it is desireable to have parity between the boundary layer thickness on

the bottom of the boat and the boundary layer thickness generated along the tunnel windows. Assuming the boundary layer experienced by a bailer on the boat can be closely approximated to that developed over a flat plate at some distance (the bailer location) aft of the plate start point, equation 3.7 can be applied and an estimate of the turbulent boundary layer thickness at the bailer location calculated. This is completed in the following table and compared to the boundary layer thickness as measured in the tunnel using a pitot tube apparatus.

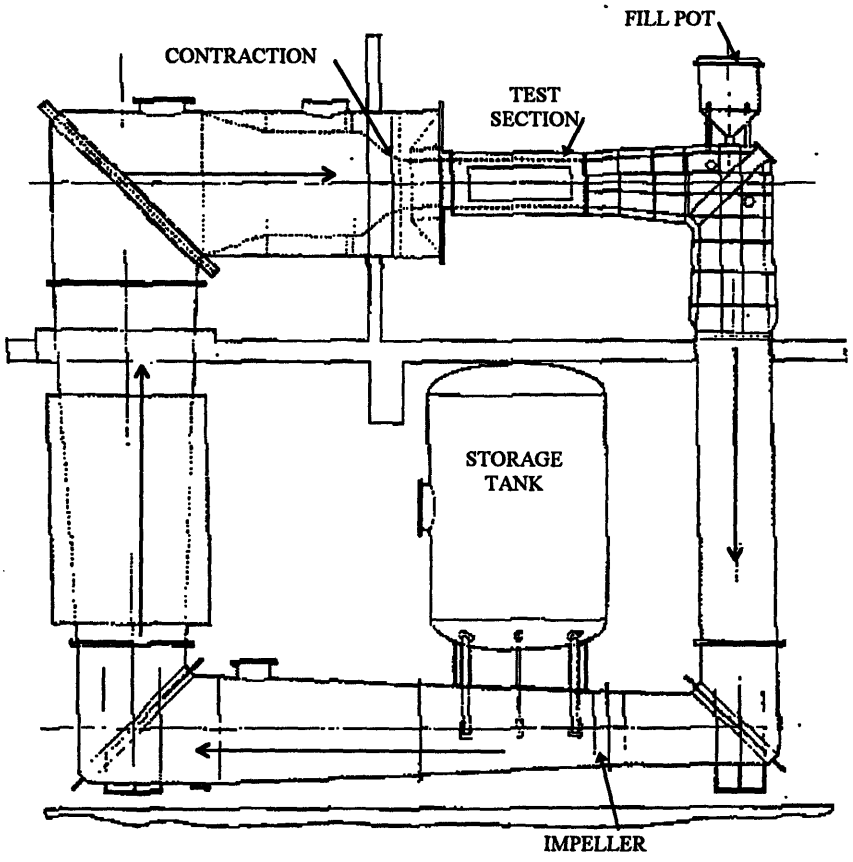

Figure 3.1 - Variable Pressure Water Tunnel Schematic

Table 3.1 - Boundary Layer Comparison

Boat	Bailer Position, m	Speed m/sec	Reynolds Number	δ, mm Calculated	δ, mm Measured [2]	Error %
Star	2.72	3.048	8.29E6	41.9	21.4	49
Soling	3.23	3.048	9.85E6	48.1	21.4	56
470	2.24	3.048	6.83E6	35.9	21.4	40

The above table indicates that the boundary layer on the boat is on the order of double the boundary layer thickness measured on the tunnel wall. This discrepancy indicates that a complete replication of actual bailer operating conditions may not be possible without direct boundary layer stimulation. Nevertheless, the consistent boundary layer thickness obtained in the tunnel allows for direct comparison between the tested bailers.

The most feasible method of determining the desired bailer performance characteristics is to develop a system where the bailer is "attached" to the top window of the tunnel with a reservoir of water stored above it. When the tunnel is operating, it simulates the motion of the bailer through the water, generating suction and causing outflow through the bailer to occur. Provided a means of obtaining time histories of the pressures at the bailer interface (the interior window surface) can be devised, all essential flow rate and minimum bailing speed variables can be measured or derived as outlined previously. A number of pressure time history measurement techniques were considered including the use of a live wire surface gauge. This apparatus uses the change in conductivity in the gauge with varying water level to obtain an electrical signal proportional to the change in water height in the reservoir. Also considered were visual means for measuring the rate of change of water level over time utilizing a camera system

and graduated manometer tubes. Finally, a series of 0 - 5 psi pressure transducers were selected both for their ease of installation and straightforward data acquisition. Of course measuring pressures at the bailer interface of infinitesimal thickness is difficult with two transducers of finite thickness and as such hydrostatic corrections were made to account for the pressure differences between the bailer interface and the centers of the transducer connections.

Because the tunnel is a closed system, only a fixed amount of water can be held in the circuit. Consequently, any water in the reservoir prior to the test must be able to be accommodated in the circuit after the run is complete. It was decided to utilize the positive pressure in the tunnel to fill the reservoir, adding no extra water to the system. The reservoir sizing is of importance for a number of reasons. Adequate volume must be stored in the reservoir prior to a test to allow the bailers performance to be characterized over time and until equilibrium is reached. Accordingly, a reservoir holding 3.2 ft^3 was adopted, rising two feet above the top surface of the top tunnel window. There must also be adequate access to the bailer from outside the tunnel to allow the bailer to be held open when filling the reservoir, for the bailer to be closed while the impeller is brought up to the desired speed, and opened once that speed is reached with subsequent data acquisition. This requirement presents an upper bound on the height of the reservoir of approximately two feet to allow a full arms length to operate the bailer. Similarly the width of the window represents another bound on the size of the reservoir such that the entire window and reservoir can be removed to allow for the tunnel apparatus to be used for other experiments.

While all of these requirements can be successfully met for the pressure measurements, the design requirements are far more complicated when drag measurements are to be incorporated. The essential design requirement in measuring the drag of the bailer using a load cell requires the bailer to be free to move in the direction of drag only. Furthermore, the bailer must be mounted in a spring type system such that when the excitation force, or drag, is applied a measurable deflection occurs. When the force is removed the bailer must return to its equilibrium or zero position to allow for consistent measurement and calibration over a particular run. This spring system must be essentially linear over the load range to be tested to enable adequate quantification of the forces being exerted on the bailer. It is the design of these springs which presents the most interesting design challenge, along with how to couple these springs and the load cell to the bailer/reservoir system.

Three separate spring systems were considered before the final design was adopted. The bailer to be tested is mounted at the base of the reservoir on a removable plate so that bailers may be interchanged without the removal of the entire apparatus. This plate and thus the whole reservoir must be free to move in the flow direction and the springs must support not only the weight of the reservoir, but also the entire weight of water in the reservoir. The springs must only deflect in motion in the stream direction and not in the vertical direction as the supported weight is varied. Any compression of the springs would result in misalignment of the bailer and the window plane, disrupting the flow around the plate and thus compromising any obtained drag results. One preliminary design incorporated the use of a set of leaf springs arranged around the reservoir/bailer

system. The reservoir would be situated within an aperture in the top window of the tunnel and the leaf springs would allow for deflection in the direction of flow. These deflections, on the order of 1/100 th of an inch, would be measured by the load cell attached to the upstream end of the reservoir on the center line and the drag data recorded. While seemingly feasible, a number of problems with this design were discovered. The effect of the varying weight in the tank would apply a great vertical load to each of the four leaf springs causing misalignment, if not failure, of the springs. Attachment of the leaf springs to both the window and the reservoir would be extremely difficult given the restrictive nature of the opening. Finally, the hole in the window must be sealed with a gasket to prevent leakage from the tunnel during experiments. This gasket must seal against a positive pressure from the water in the tunnel and must not affect the linearity of the spring system which could dramatically alter the results.

The potential for non-linear effects on system response due to gasketing materials was also the reason for dismissal of the second suggested design. In this case, in place of the leaf springs, the bailer reservoir system would be supported by a rectangle of one inch thick rubber or neoprene, so that drag on the bailer would force the rubber to deflect in torsion. The major problem with this system is the non linear deflection of the neoprene foundation which would dramatically compromise the results. Also, the nature of the foundation would make compression under the reservoir weight likely, displacing the bailer to a position below the plane of the window. The requirement of restraining the reservoir's motion in all but the desired stream-wise direction would also be difficult and

would require the use of external restraints, further affecting the stiffness of the entire system.

The final apparatus design as depicted in Figures 3.2 and 3.4 has eliminated a number of the problems identified above and utilizes a series of three vertical compression rods and two horizontal rods to prevent twisting of the entire mechanism. These rods are made of steel and contain two necked down regions (Figure 3.3) that allow the apparatus to deflect under load in the stream wise direction but are rigid in the vertical plane: largely eliminating the difficulties with compression due to the variable reservoir loading during operation. As in the previous designs the bailers are located in removable plates. These plates allow ample room for a variety of bailer geometries to be tested and are mounted into a flange at the base of the reservoir using a neoprene compressible gasket to seal the bailer from flow through areas other than the bailer outlet. Following the design constraints in regard to reservoir dimensions, the reservoir extends vertically to a height of 24 inches allowing for access for bailer operation and providing an adequate head for testing. Width and length of the apparatus are limited by the accessible window area inside the window sealing flanges and further restricted by the requirement that the compression rod and torsional restraint foundations be located within the accessible window area. Similarly, adequate space on the window must be allowed for load cell mounting and access. To provide for the necessary volume in the reservoir and to incorporate the space requirements of the torsion and compression rods the reservoir profile is of a T-shaped section with the bailer mounted at the base of the T stem and the test section being the full width of the T. This necking out of the section is located three

inches above the top window plane to allow for hand access and to provide for the torsional restraints to pass underneath the test section. The three compression rods attach to the reservoir section along a flange plate welded to the sides of the reservoir. These rods are then coupled to studs that are embedded into the window providing a solid support for the rods and the reservoir. The torsional restraint rods are bolted through plates welded to the base of the test section and the remaining ends attached to aluminum angle foundations, rigidly bolted to the window. All rod connections are threaded to allow the apparatus to be leveled in attitude and aligned with the free stream.

This final design eliminates difficulties with compression under varying weights of water in the reservoir and provides for a simple means of adjusting the orientation and location of the bailer. The nature of the necked down compression rods creates a series of three springs which deflect only within the linear range of the steel removing any difficulties with non-linear stiffness variations over the small range of deflections encountered. The 5 pound load cell is connected to the apparatus in a fashion similar to that of the torsional restraint rods with an aluminum angle foundation bolted directly into the window. The load cell probe is through-bolted to a plate welded at center line on the upstream edge of the reservoir below the test section.

As with the other proposed designs the reservoir and bailer plate are positioned in an aperture in the top window of the propeller tunnel. When the tunnel is operating, water in the test section is under a positive pressure and thus a means of sealing the quarter inch gap between the window and the reservoir system must be devised. To facilitate this an aluminum flange was added to the reservoir at the top window level to provide a sealing

point for the gasket on the reservoir. Studs were positioned in the window to provide an anchoring point for the gasket.

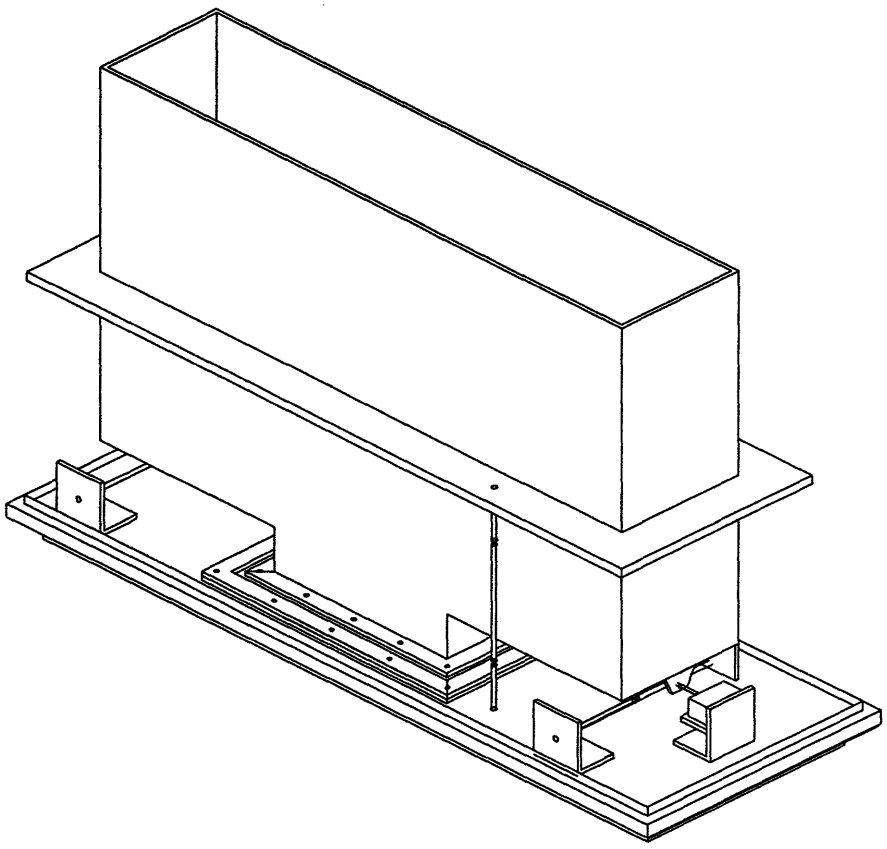

Figure 3.2 - Apparatus Isometric View

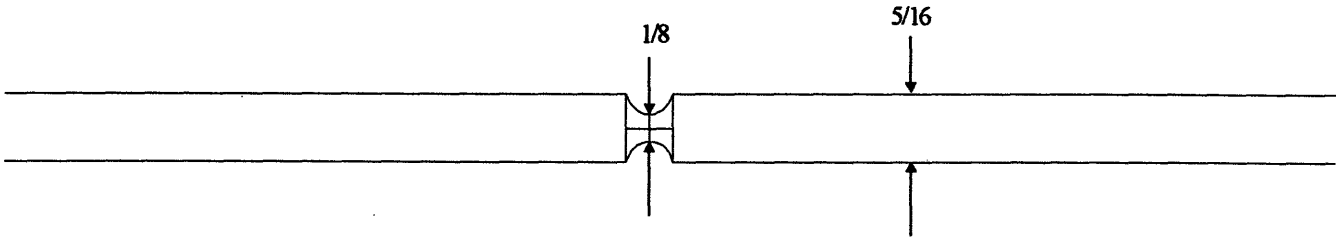

Figure 3.3 - Compression/Torsion Rod Details

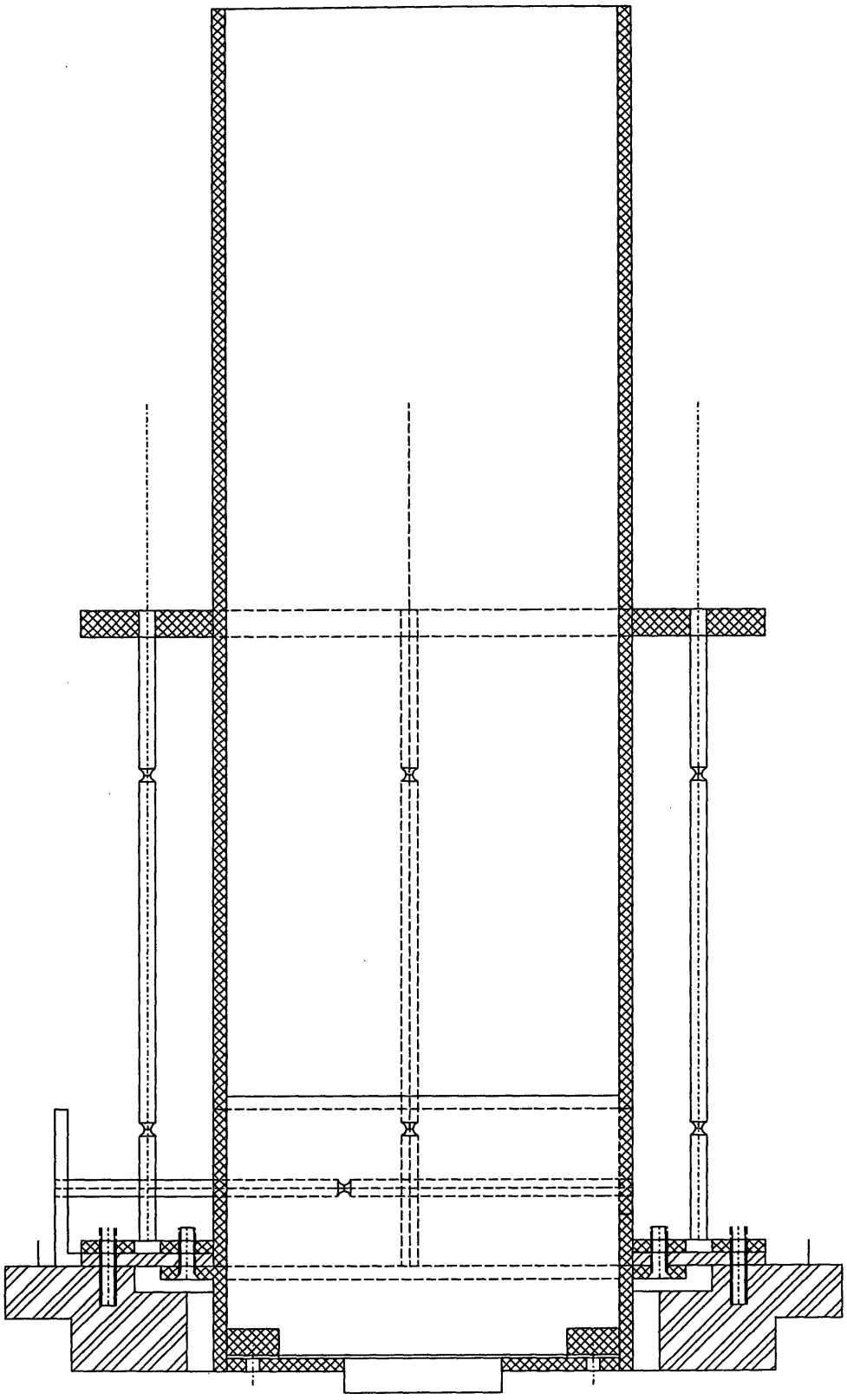

Figure 3.4 - Experimental Apparatus Cross Sectional View

A gasket of natural rubber was then stretched over the reservoir flange and the window studs and aluminum plates fastened over the gasket to the studs to complete the seal. The quality of the seal was shown to be a function of the material chosen for the gasket and after eliminating a variety of rubber seals, a stiff latex sheet gasket was adopted. Other difficulties directly related to the type of gasket material used are dealt with subsequently.

A pressure sensor was positioned in the side wall of the reservoir below the test section at a position four inches above the bailer plane. To provide for a visual check on the water pressure read by the reservoir sensor and to allow for calibration procedures, a sight glass and meter stick were fitted to the outside of the tank such that the center of the sight glass inlet was at the same elevation as the center of the pressure sensor. Tunnel pressure was measured by an identical sensor located at a known distance below the bailer interface and connected by tubing to the tunnel stream via two pressure taps in the side wall of the tunnel. These two taps were located at midstream height and at opposite ends of the tunnel test section to provide the average pressure over the length of the test section. The overflow pot at the downstream end of the tunnel is fitted with a permanent sight glass and by fitting a meter stick along the sight glass at a known vertical location in relation to the pressure sensor, a visual measurement of the pressure seen by the sensor at zero flow speed can be made.

Originally, concerns that the equilibrium pressures at the testing speeds could not be reached with the available head difference above the bailer lead to the investigation of a reservoir design with a closed top such that a vacuum could be applied and the pressure in

the reservoir adjusted. Preliminary tests indicated that at the desired testing speeds all bailers would reach an equilibrium point without ventilation occurring and while the water level in the reservoir remained within the test section region. The use of a vacuum system was not investigated any further.

3.4 - Data Acquisition

Electronic data acquisition was used to record time histories of both reservoir and tunnel pressures and in obtaining drag measurements. The pressure sensors selected were Omega PX26-005DV Differential Pressure Transducers of the four-active piezoresistive bridge type. These transducers were configured such that one side was directly linked to the pressure port to be measured while the other was vented to the atmosphere. While a single transducer could be used to measure the differential pressure across the bailer directly, the use of two separate transducers eliminated difficulties in bleeding air from the sensor inlet tubes. Each transducer was supplied with 15V DC excitation with output to an operational amplifier through a low pass L-C circuit filter whose output was connected to the PC's data acquisition board.

The selected load cell was an Advanced Mechanical Technology, Inc. (AMTI) FD-1-0500 tension/compression load cell with a five pound load range. The selected load cell is based on Hall Effect devices coupled with a precision magnetic displacement system having a rated full load displacement of 1/100 th of an inch (250 microns). While this load cell has integral signal conditioning it was important that all signals fed to the data acquisition board were delayed by the same time constants. Because of this, the load cell signal was conditioned by a low pass filter with the same time constant as the pressure

sensors. The small range of loads to be measured and the violent nature of the bailer opening and closing process requires that considerable attention be paid to the overload capacity of the load cell. The AMTI load cell selected has an overload protection of 1000% which is more than adequate for the anticipated maximum loading.

A Metrabyte DASH - 16 analog/digital data acquisition board installed in an IBM compatible personal computer was used to convert the sensor output signals to digital format, time history signals at a sampling rate of 20 Hz. This data was then recorded utilizing a custom data acquisition program written as part of the 1996 Independent Activities Period Class "Design a Better Bailer". This program records all three sensor channels along with calibration information, computes the calibration constants and converts the acquired digital signal to calibrated units. Both raw data in the form of counts taken from the DASH - 16 board and calibrated output are written to files for subsequent plotting or further post processing and non-dimensionalization.

Chapter 4 - Experimental Procedure

4.1 - Methods of Calibration

For both pressure and load cell sensors the quantity measured is represented by a voltage reading such that when pressure or load is applied, a different output voltage, linearly proportional to that quantity is produced. The analog to digital converter converts the voltage signals from the sensors to digital values which are directly proportional to the voltage, the digital values are then written to a computer file. Calibration provides a means of determining the proportionality constants and thus converting the readings to quantities of physical relevance. Provided the sensors are linear over the required range, recording a sensor's electrical output and a known value of the physical parameter being measured at at least two points presents a means of calculating these proportionality constants. In fitting a linear equation through the known points, the gradient of the equation becomes the factor relating the known voltage to the physical variable, while the offset of the line from the origin represents a zero shift in the sensor reading, i.e. zero voltage does not correspond to zero pressure or load.

A means of alternatively determining the correct value of the physical parameter at the two calibration points must be available. In the case of the pressures, the two sight glasses can be used to read the height of the column of water above the center of the sensor and consequently the pressure can be calculated. In the case of the load cell, hanging known weights from the load cell provides a means of applying known forces and establishing the required data points for calibration. The data acquisition program records

sensor readings in digital "counts" at user entered reservoir and tunnel heads, automatically calculates the pressures represented by these head readings and determines the required calibration constants. These head readings and all sensor readings are automatically corrected for the sensor and sight glass offsets from the bailer interface plane.

Integrating the calibration with the testing procedure can dramatically reduce the time required to complete the experiment and improve the accuracy. For this reason a pressure calibration point was obtained with the reservoir full prior to bringing the tunnel up to speed and after the experiment, once the bailer had been closed and the tunnel speed had returned to zero. By waiting until the tunnel speed had returned to zero it was insured that both calibration points were obtained reading only static pressures. By bounding the experiment with the calibration points any significant shift in zeros during the run of the experiment would be clear in a plot of the pressure traces and that run could be repeated immediately. Force calibrations were completed at one time by hanging three known weights, routed by pulleys, from the apparatus as shown in Figure 4.1.

It is important to note that this arrangement for calibrating drag provides for the effects on the system's spring stiffness from both the compression and torsion rods and the gasket's elasticity. Provided the pulley system is arranged so that it supplies force only in the drag (stream) direction and that the friction due to the pulleys is negligible, the voltage registered by the load cell will directly correspond to the force applied from the weight of the string and applied weights, automatically accounting for the entire system's stiffness.

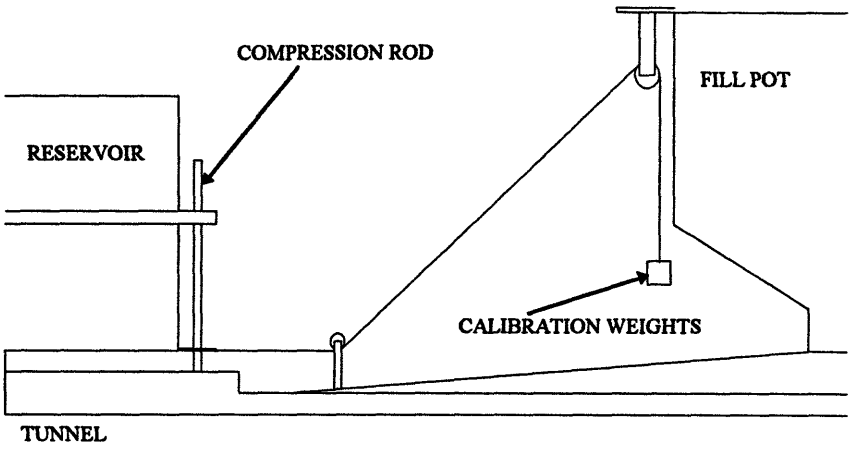

Figure 4.1 - Force Calibration Arrangement

4.2 - Original Test Procedure

As constructed, the experiment was designed to measure both pressure and drag characteristics over the duration of each experimental run. For this case the following procedure was devised:

1. Begin tunnel filling procedure.
2. Open the bailer and hold open any check valve mechanism filling the reservoir to the point that water levels in both the reservoir and overflow pot can equalize and the reservoir will not overflow.
3. Close the bailer.
4. Bleed tunnel pressure sensor tube to eliminate air bubbles that may cause erroneous results due to the effect on hydrostatic pressure.
5. Read the tunnel head from the sight glass and input into the data acquisition program.
6. Read the reservoir head from sight glass and input into the data acquisition program - Completing the first pressure calibration point.
7. Apply a known calibration weight to the reservoir system and enter weight value into the data acquisition program.
8. Apply a second weight to reservoir system and enter value into data acquisition program - Completing drag calibration.
9. Bring tunnel up to desired testing speed.
10. Open bailer and begin acquisition.
11. Once data acquisition and equilibrium is achieved visually record the equilibrium head difference from the manometer tubes.

12. Close the Bailer.
13. Turn speed off.
14. Once speed at 0, read tunnel head and enter into data acquisition program.
15. Read tank head and enter into data acquisition program - Second calibration point completed.
16. Plot data pressure and drag traces and confirm and starting and finishing values.
17. Repeat for next speed and all other bailers.

The procedure outlined above was designed to facilitate coupled measurements of both pressures and drag readings, allowing the examination of the effects of decreasing flow rate on the magnitude of the drag measurements. To confirm that such coupled measurements were possible a series of experiments was completed. These experiments involved recording load cell readings as the reservoir water level was increased. All tests were completed with the reservoir apparatus removed from the tunnel such that the obtained drag readings were solely a function of the varying reservoir water level, without the effects of tunnel speed. Figure 4.2 shows non-linear variation in the measured drag readings as a function of the water depth, eliminating the possibility of calibrating this change and applying a known correction to the obtain drag measurements. Figure 4.2 indicates a variation of up to 8 Newtons in drag measurements as the water level varies over the height the reservoir, a value much greater than the 2 to 4 Newtons expected from bailer drag alone.

This phenomena can be attributed to a number of factors linked to the construction of the experimental apparatus. As the water level drops, the position of the center of gravity of the reservoir and the water contained in it also varies, not only vertically as expected, but also in the longitudinal and transverse planes. The apparatus was originally

designed so that the weight of water would be isolated in the vertical compression rods and only the longitudinal drag force would be transmitted to the load cell. Whether through anomalies in the apparatus construction, varying stiffness in the compression rods or misalignment of both the reservoir and the compression rods, this was not the case as is clearly seen in Figure 4.2. Because of these construction anomalies and gasket non-linearities the varying position of the center of gravity causes deflections of different magnitudes in the compression rods. As a result, the water weight is not uniformly supported by the rods and a moment is created about the load cell. This results in a drag measurement being registered.

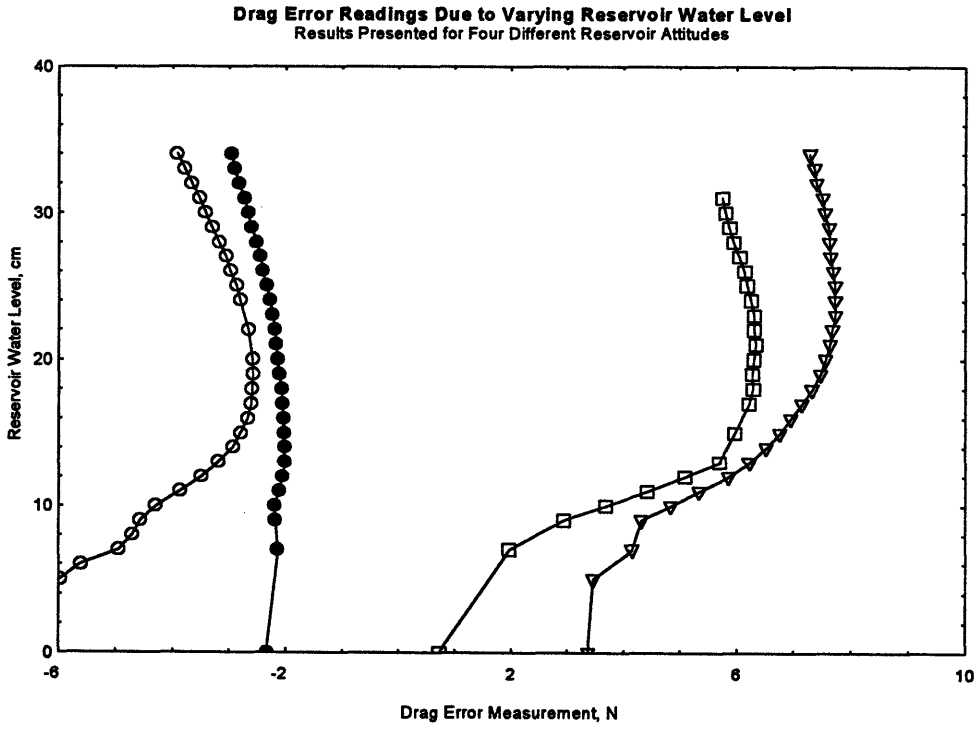

Figure 4.2 - Load Variation With Decreasing Reservoir Water Level

In theory, correct alignment of the apparatus and compression rods should allow the entire weight force of the water to be isolated in the compression rods leaving only the drag

translation to be resolved by the load cell. To investigate the effects of the apparatus alignment identical tests were repeated at different attitudes. In no case was an alignment found that brought the variation within an acceptable margin of the expected bailer drag and an alternate drag measurement experiment was devised.

4.3 - Drag Experiment Correction and Final Testing Procedure

With the observation that coupled time measurements of both the drag and the pressures is not possible, an alternate procedure must be defined. Application of the conservation of momentum equation to the bailer control volume leads to the conclusion that the maximum drag experienced by a deployed, non ventilating bailer will occur when no fluid is being ejected from the bailer and the check valve mechanism is closed. In this case there is no contribution of momentum flux to the system from the ejected flow and thus the entire momentum deficit across the bailer is represented in the drag measurement. Following this argument it is expected that the drag of the bailer will be at its lowest when the flow rate is at its maximum value. The drag is expected to increase as the flow rate decreases to the no-flow equilibrium point. The outflow in the ventilating condition is very chaotic in form and the unstable nature of the flow makes it difficult to characterize the drag in this condition. By testing the fully deployed, no-outflow drag of each bailer prototype, a comparison of the drag characteristics of the bailers would be possible.

Incorporating these observations, the original procedure was altered to consist of two separate experiments, one for pressure testing and a second for drag measurement. The pressure testing procedure is identical to that outlined in Section 4.2 with the removal of steps 7 and 8 concerning the calibration of the load cell. Following the observations

concerning the drag error as a function of changing reservoir water level, the ideal drag test consists of a dry reservoir and a sealed bailer so that in the deployed condition no inflow can occur. Such a test relies on the effectiveness of the bailer check valve mechanisms which often fail to completely seal in operation. This problem is exaggerated in those bailer prototypes where no check valve mechanism was incorporated and requires the use of a manually fitted plug to prevent inflow. Examination of Figure 4.2 shows that the greatest drag error occurs at the higher water levels and steadily decreases in magnitude as the water level drops. At the lowest water levels the magnitude of the drag error is small in part because this region is below the first compression rod notch limiting any uneven rod deflections. Provided the water level is kept in this region, drag data can be obtained with confidence. In the case of closeable production bailers concerns over the amount of water in the reservoir are eliminated as only minor leakage occurs. However, in the case of the prototype bailers, many of which were constructed without closing mechanisms, the leakage is largely a function of the ability of a weighted plug to seal under operation.

In light of this, a procedure was adopted to minimize the amount of water in the reservoir. For those bailers that could not be closed the tunnel was brought up to sufficient speed to cause ventilation to occur. Once ventilating, a weighted plug was positioned over the bailer inside the reservoir, the speed reduced to the desired test speed and data acquired. Visual observation of the apparatus operating lead to the conclusion that the drag readings obtained from the load cell included not only the drag of the bailer but also the drag of the reservoir in the aperture. The half inch gap between the reservoir

and the window affects the flow over the bailer installation plate. Despite positioning a flow fairing tape over the gap (but not touching the reservoir) the drag measured includes a component of drag related to the reservoir apparatus and not to the effect of the bailer. To obtain a measurement of the drag of the bailer alone, a determination of the tare drag must be made before the flow is perturbed with the bailer. For every closeable bailer, calibration with zero speed and the bailer retracted was completed by hanging a series of three known weights and repeating the zero reading before and after the weight hanging. The tunnel was then brought up to the specified test speed and data acquired for a minute and averaged to give a value of the drag for the reservoir and retracted bailer tare. Once the tare values had been recorded the bailer was then deployed and data obtained over a minute duration for the no outflow drag condition. This data was also averaged and the resultant drag of the bailer determined by subtracting the tare from the drag values. At 12 feet per second a dynamic calibration was completed by applying weights to the apparatus with the bailer retracted. An average of the gradients obtained from least squares linear curve fits of both the static and dynamic calibration data points was used to convert the load cell output to bailer drag. A series of three weights were used in the calibration.

Of course those prototypes that are not closeable present difficulties, not only in sealing the bailer from inflow, but also in the measurement of bailer tare and applying consistent calibration values across each experiment. The best solution to this problem lies in the construction of prototype bailers capable of closing. However, this presents large expense and in many cases an engineering challenge that was outside the scope of this work. To allow for determination of drag results for these prototypes, experiments were completed in such a way that a production bailer was tested followed by a non-

closing prototype. In this way calibration constants and tare readings from the production bailers were adopted for use in interpreting the non-closing prototype drag measurements. While such a solution to the problem is inexact, the obtained results serve to give a reasonable estimate of the bailer drag. To improve accuracy of the measurements all production bailers, with the exception of the Super Max bailer, were retested at least twice along with the most promising prototype bailers. Clearly erroneous results were eliminated before averaging the remaining values and non-dimensionalizing. A detailed discussion of the drag results is provided in Chapter 7.

Chapter 5 - Bailer Prototypes

5.1 - Production Bailers

A series of five production bailers manufactured by Andersen of Denmark were selected to provide a series of baseline data for varying geometric configurations. Although these bailers exhibit the same general geometry depicted in Figure 2.1, they are not scaled models and hence testing these production bailers provides a simple means of investigating the effects of varying length, outflow hole size and geometry, face plate width and channel size.

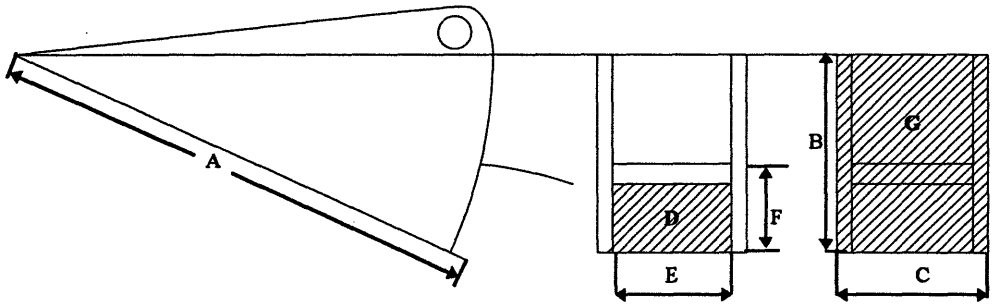

Figure 5.1 - Critical Bailer Dimensions

Table 5.1 provides the dimensions of the bailers as shown in Figure 5.1 illustrating the differences between the production bailers.

Table 5.1 - Production Bailer Dimensions

Bailer	A	B	C	D	E	F	G
Super Mini	6.168	2.780	2.490	6.80	1.442	1.940	2.797
Mini	6.940	3.258	3.530	11.50	1.482	1.902	2.819
Super Max	8.766	4.104	3.582	14.70	1.710	3.162	5.407
New Large	9.932	4.792	3.902	18.70	1.840	2.500	4.600
Super Medium	8.786	4.252	2.540	10.80	1.850	2.140	3.959

Dimensions A,B,C,E,F in cm Dimensions D,G in cm^2

From the table it is clearly seen that a reasonable variation in geometric quantities is present between the various models. By testing the production bailers, an indication of the relative effect of a number of geometric factors on the performance of the bailer can be made.

5.2 - New Prototype Bailers

While the testing of production bailers can illuminate the relative merits and drawbacks of the traditional bailer design, it is possible that a completely different geometric form would produce considerable benefits in one or more of the areas of concern. For instance, much work has been done in the development of low drag shapes with known pressure distributions for use in both marine and aerospace applications. By adapting these shapes it may be possible to create a bailer form that has a greater flow rate, operates at a lower speed and has a lower drag than the current designs.

As outlined in Chapter 2, the general principal governing bailer operation lies in the perturbation of the flow field around the bailer. As the flow is accelerated around the bailer a region of low pressure is created behind the bailer face drawing the water out. The magnitude of the fluid acceleration was explored in Chapter 2 and can be related to the non-dimensional pressure coefficient by the following equation:

$$-Cp = 1 - u^2/U^2 \qquad \text{Equation 5.1}$$

Where,

u = *perturbed velocity*

U = *free stream velocity*

If a pressure coefficient for the production bailers can be determined, this value can be used as a target C_p for a new geometry. Any bailer exceeding this C_p should theoretically

generate a lower suction pressure and will consequently achieve a greater outflow rate and a lower bailing inception speed. From Table 2.1 it can be seen that for the Super Medium Bailer considered an approximate ratio of the perturbation velocity to the free stream velocity was determined. Substituting $V_1/V_2 \approx 1.18$ into Equation 5.1 we can calculate the bailer's C_p.

$$Cp = -(1 - u^2/U^2) = -1 + (1.18)^2 = 0.39$$

Hence, any bailer exceeding a pressure coefficient of 0.39 should have a greater flow rate for its size than the current production bailers.

5.2.1 - Hydrofoil Bailer

Airfoil sections such as those developed by the NACA are commonly used in the design of yacht appendages including, keels, rudders and centerboards. These appendages are essential for boat control, contribute to the stability of the vessel and act to prevent the vessel slipping sideways as a result of components of hydrodynamic and aerodynamic lift. Utilizing the low drag nature of a foil section and incorporating the desired pressure characteristics presents several interesting possibilities for a bailer design. The first prototype was constructed using a hollow NACA 0024 foil section having a pressure distribution as pictured below in Figure 5.2 [1].

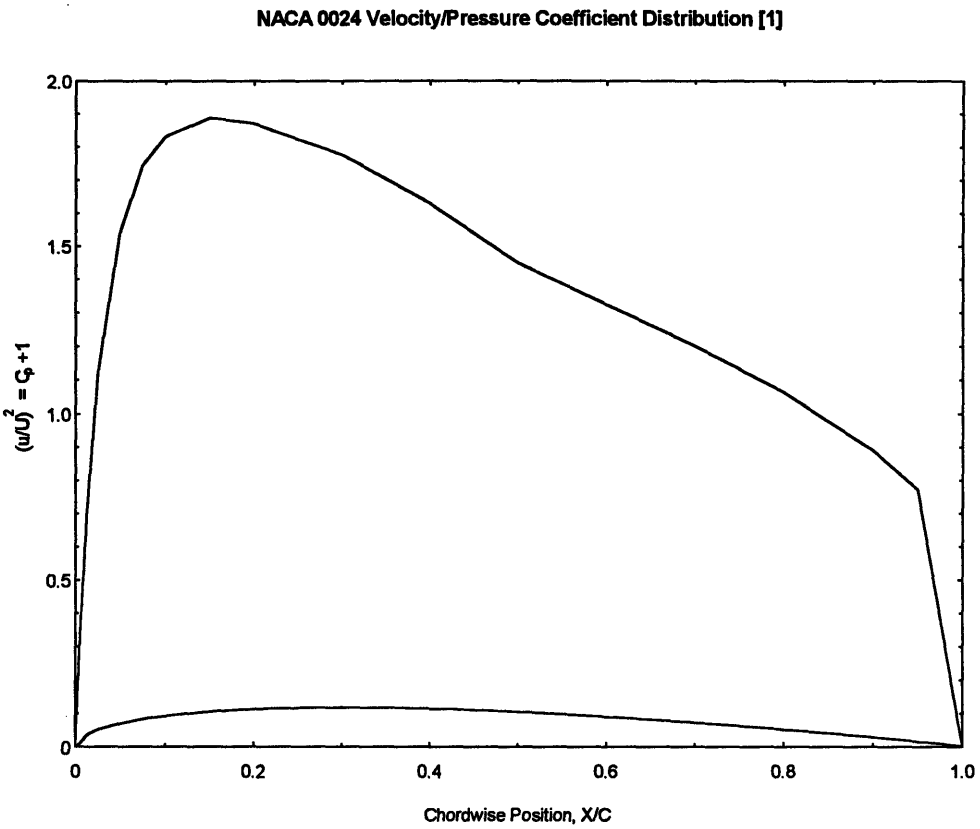

Figure 5.2 - NACA 0024 Pressure Coefficient Distribution

As originally envisioned the bailer would consist of a fully retractable foil of constant section terminating at an endplate serving two purposes: To reduce end effects on the foil and to provide a flat surface to seal with the bailer housing in the retracted position. At some position along the foil chord a slit or series of holes running the entire span of the foil would be placed so as to allow for the flow of water out from the bailer. This bailer is depicted in Figure 5.3. The position of the holes or slits was determined from the pressure distribution such that the minimum pressure (suction) was available to obtain the largest possible outflow. To ensure tangential outflow from within the foil housing an interior fairing was implemented as shown in Figure 5.4.

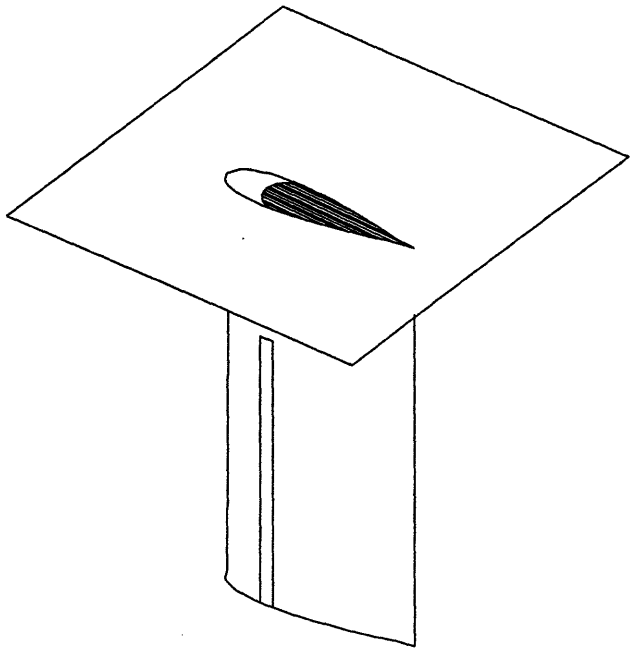

Figure 5.3 - Hydrofoil Bailer

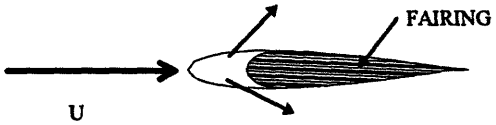

Figure 5.4 - Hydrofoil Bailer Interior Fairing Detail

A variety of means of preventing back flow into the bailer were suggested for those cases where low speed produced insufficient suction for operation. These included the use of flexible flaps over the slits/holes so that when no outflow occurs they seal flush against the foil. Also suggested, was the use of a check valve at the inlet to the bailer

inside the boat. This method would eliminate complexity external to the boat but the effects of the open slits on the drag of the bailer, particularly when the bailer is not operating would be pronounced. A final determination of the best check valve method was delayed until a measurement of the merits of the designs could be achieved.

The hydrofoil bailer presents some interesting possibilities for the use of the bailer in keel boat vessels where the outflow passages could be incorporated directly into the keel design. Such an application is of course dependent on the relative merits of the bailer as compared to more traditional production bailers.

5.2.2 - Blister Bailer

In developing a low drag body with the requisite pressure characteristics it was surmised that a lifting body or blister fitted to the hull would perturb the flow and create suction without the penalties associated with the tip vortices on the hydrofoil. Unlike the foil sections where a design section's properties are readily available, the determination of a desirable body shape for a three dimensional lifting surface is more difficult. To facilitate the development of a body achieving the lowest suction pressure without separation a research computational fluid dynamics code was utilized. This code is an axisymmetric potential flow solver using source and dipole rings in a Green's formulation panel method to solve for the potential flow about the body. This solver is coupled with a viscous flow solver from which determination of the separation characteristics of the selected shape was made. Of course this bailer must be modeled with its interaction with the hull form. For potential flow, application of the method of images leads to an accurate model of the body

and interface. As the bailer is half of an axisymmetric body, its image is the remaining half and the axisymmetric code can be applied successfully.

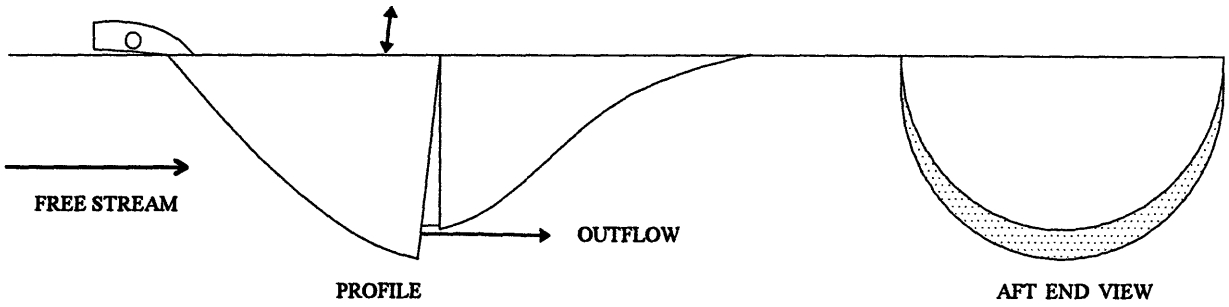

Figure 5.5 - Blister Bailer Prototype

A variety of shapes were numerically tested to determine a form with the desired pressure properties and with a shape promoting attached flow. After iterating through a variety of shapes a final testable form was realized and this shape constructed over a male mould from fiber glass before being finished with fairing compounds. The final design is depicted in Figure 5.5 and has been characterized as the Blister bailer as in the non-bailing condition the bailer forms a faired protuberance on the hull. As originally envisioned the forward portion of the blister is hinged at the apex of the body so that in favorable pressure conditions this portion drops down creating an opening at the point of minimum pressure through which outflow will occur. Ideally this bailer will open automatically in favorable conditions and will close when the suction is inadequate, eliminating the need for additional check valve mechanisms.

The current generation of bailers is designed so that when retracted they seal flush with the hull inducing no additional drag. In the case of a permanently deployed Blister an increase in the drag experienced by the yacht must necessarily occur, considerably detracting from any advantages to be had from this bailer form. A number of suggestions

including the possibility of rotating the blister into the boat so as to produce a flush surface when not in use, or incorporation of a sliding mechanism to replace the blister bailer with a flush insert were considered but implementation was delayed until the relative merits of the Blister bailer had been determined.

5.2.3 - Membrane Bailer

Following the intuitive notion that a faired body presented to a flow will induce less drag it was sought to design a retractable bailer of similar geometric proportions to the production bailers outlined previously. By replacing the body of the bailer with an elastic membrane that is taught and flush with the hull of the boat when not in use, but can deform to a faired leading edge shape to perturb the flow a combination of the Blister and production bailer designs was achieved. The rubber membrane is taughtly attached to the hull on the outer and upstream edges, with the downstream edge free to deform such that the membrane is flush with the hull when retracted. A moveable metal U frame is attached to the center of the downstream edge of the membrane such that when forced down the shaped frame deforms the membrane creating a fair body as depicted in Figure 5.6.

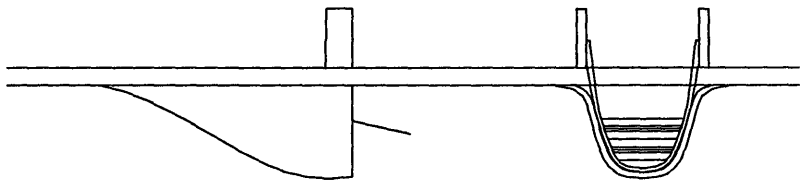

Figure 5.6 - Membrane Bailer

This frame may include a check valve door to limit the back flow when insufficient suction occurs. While the theory behind this bailer is sound, application of these ideas presented great difficulties, particularly in finding materials of the desired elasticity and in attaching the membrane to the bailer. These problems in construction were not successfully solved and a working prototype was never completed for testing.

In association with Mr. Matthew Tobriner of Science Applications International Corporation a prototype bailer incorporating many of the features of the membrane bailer was developed but was not completed in time for testing to be carried out. In this proposed design a spring stainless steel membrane, triangular in planform was substituted for the elastic membrane such that downward deflection of the spring steel by a U frame device would present a faired body to the flow reducing the drag. This apparatus was designed so that lifting a plate over the top of the bailer would push the U frame into position opening the bailer. When the lid was closed and bailer retracted any leakage through the unattached end of the bailer would be prevented. It should be noted that the size of this bailer is particularly dependent on the strength and ductility of the spring steel used and the ideal geometric configuration, particularly with regard to depth of protrusion may be unattainable.

5.3 - Modifications to Production Bailers

As discussed previously, the production bailers tested exhibit a variety of geometric variables within the same general form. To systematically consider the effects of the major design features on the performance of production bailers a Super Mini

Andersen production bailer was chosen as a control and a series of modifications made to identical bailers.

5.3.1 - Doorless Bailer

Consideration of the bailer dimensions in Table 5.3 shows that the actual outflow area is restricted to a small region at the aft end of the bailer, in all cases less than half of the available depth in fully deployed operational mode. Reasons for this include: strength considerations, ease of incorporating a check valve door, or following the fact that the greatest velocity and therefore greatest suction will occur at the lowest extremity. This may be particularly true in light of the boundary layer profile along the bottom of the boat. An experimental check on the actual performance effects of restricting this area was sought and so the entire aft face of a Super Mini bailer was removed, including the check valve door. The resulting bailer was found to have sufficient structural strength. In subsequent sections this bailer is referred to as the "Doorless" bailer.

5.3.2 - Sideless Bailer

Similar reasoning leads to questioning the importance of the side channel walls on the bailer performance. To investigate this, a Super Mini bailer was welded in the open position such that the face plate was maintained at the same angle as in the fully deployed production version. The side and aft walls were then removed so as to leave a flat plate inclined to the flow. Custom sealing mechanisms were created for closing the bailer during pressure and drag tests. This bailer is referred to as the "Sideless" bailer in subsequent sections.

5.3.3 - Faired Bailer Inlet

Also of interest is the effect of fairing the bailer inlet. While this region has no effect on the external hydrodynamics governing the performance of the bailer, any head losses in the interior flow of the bailer will adversely affect the flow rate. To investigate this phenomenon a foam fairing was fitted around the locking mechanism of a Super Medium Andersen bailer as shown in Figure 5.8. In this case no modifications to the bailer structure were made.

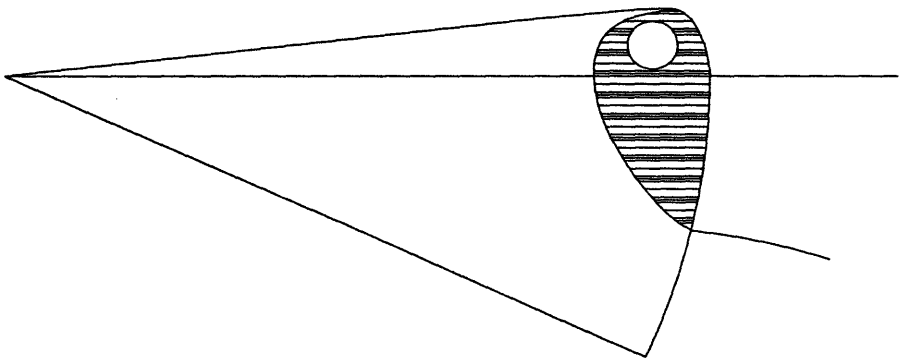

Figure 5.7 - Super Medium Inlet Fairing

Chapter 6 - Bailer Flow Rate and Bailing Inception Speed Results

6.1 - Pressure Data Reduction Methods

As outlined in Section 3.4, all signals are initially processed using a low pass filter before being acquired by the personal computer. This filter acts as a first stage of smoothing but examination of a low pass filtered, raw data trace such as that depicted in Figure 6.1 indicates a great deal of noise in the tunnel pressure reading and consequently in the pressure difference reading.

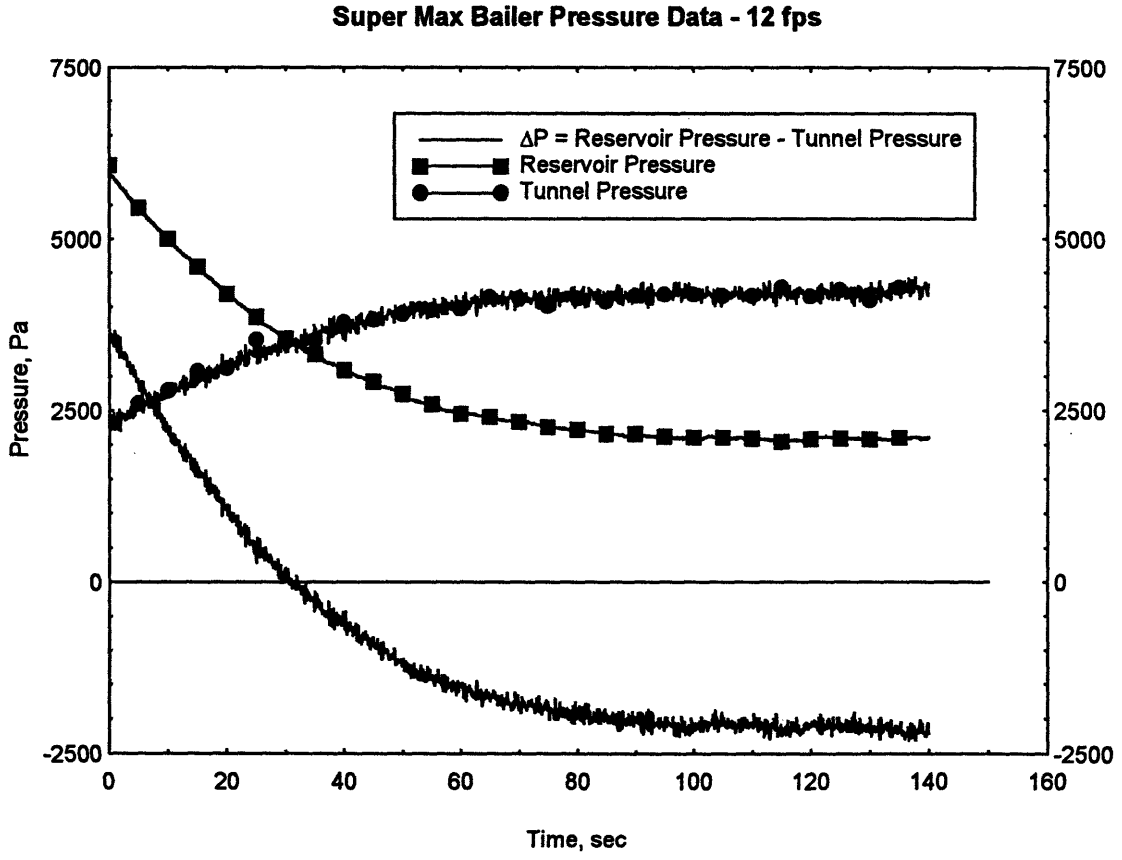

Figure 6.1 - Raw Pressure Data

Further post processing of the results was used to eliminate this noise and allow for a better representation of the obtained data. The smoothing of these pressure traces is

of particular importance in determining the pressure difference and in calculating the flow rate by taking the derivative of the reservoir pressure trace. To achieve this, a post processing routine was written to replace the raw pressure traces of the type depicted in Figure 6.1 with a 100 point moving average of the data. Figure 6.2 shows the post processed pressure traces for the Super Max production bailer. These traces are considerably smoother than the original data, improving the ability to resolve the flow rate characteristics of a particular bailer.

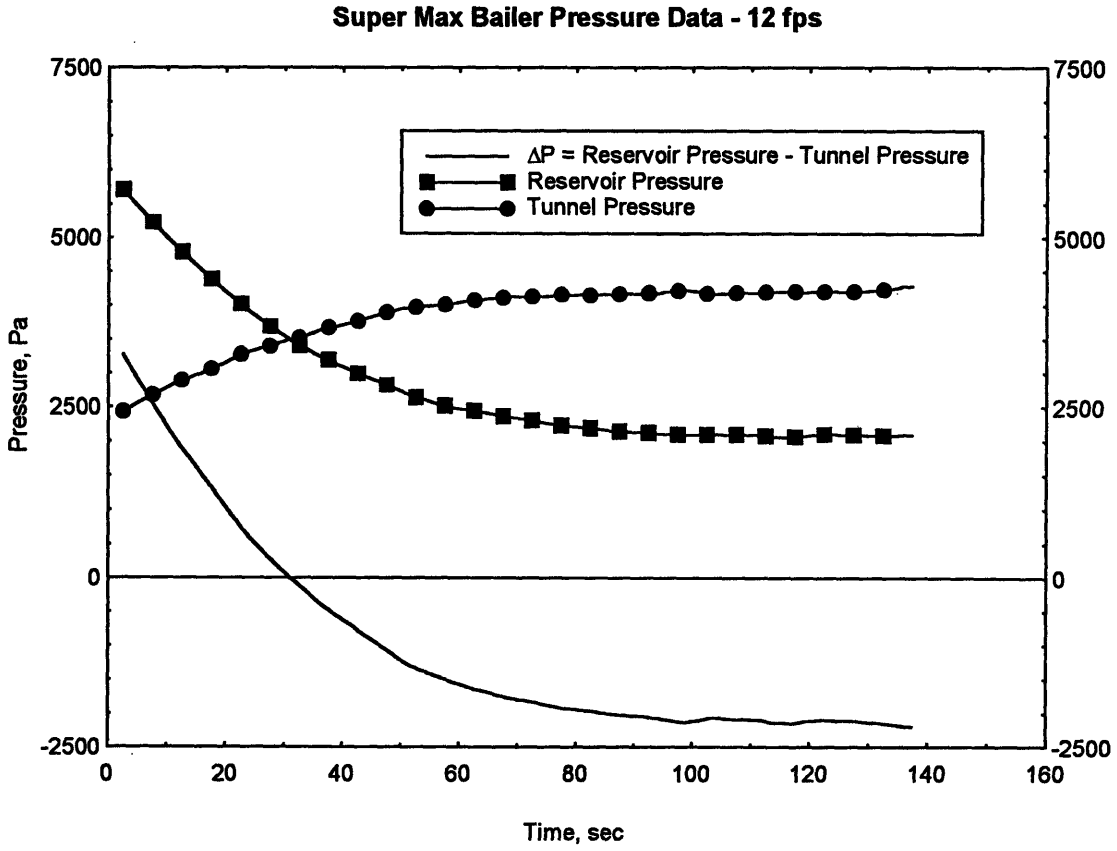

Figure 6.2 - Post Processed Pressure Data

While the moving average dramatically smoothed the pressure traces, the size of the data files remained large, due to a sampling rate of 20 Hz and an experimental run of two minutes leading to 2400 data points for each acquired channel. This large number of data

points does improve the accuracy of the pressure curves, but creates major difficulties in memory allocation for the graphic display of the data and more importantly in the numeric determination of the flow rate. According to equation 3.1 the volumetric flow rate of the bailer at a particular speed is directly proportional to the time derivative of the reservoir pressure trace. A number of means of determining this derivative were considered. Firstly, a variety of functional forms were fitted to the reservoir and pressure difference data such that an analytic determination of the derivative would be possible. From a visual examination of the pressure traces it is apparent that the flow rate should monotonically decrease until zero flow rate occurs at the equilibrium condition. In many cases the functional form did not exhibit this requirement creating some difficulty in resolving the minimum operating pressure and corroborating this value with the visually recorded data. In some cases, success was achieved using a least squares fit of a power law of the form:

$$P = at^b + c \qquad \text{Equation 6.1}$$

This law and the exponent were not uniformly applicable across all recorded data sets and a numeric rather than analytic means of determining this derivative was adopted. Even with the 100 point moving average smoothing, oscillations are still apparent in the data. Consequently, application of a Euler central differencing rule in the calculation of the derivative at the central point results in inconsistent and often violent oscillations in the calculated derivative. By replacing a second's duration of data points (20 points) with their average a number of problems were alleviated. Firstly, the use of a central differencing rule was acceptable as it utilized points of adequate separation to better capture the trends evident in the data. It must be noted that some significant oscillations

are still present in the resulting curves. However, it was felt that any further reduction in the number of data points would compromise the validity of the results. Secondly, this replacement scheme sizably reduced the number of points in the data sets easing any memory constraints and improving other post processing procedures. As shown in Figure 6.3 below, the essential character of the calculated non-dimensional flow rate trace is unchanged through use of the 20 point replacement averaging method.

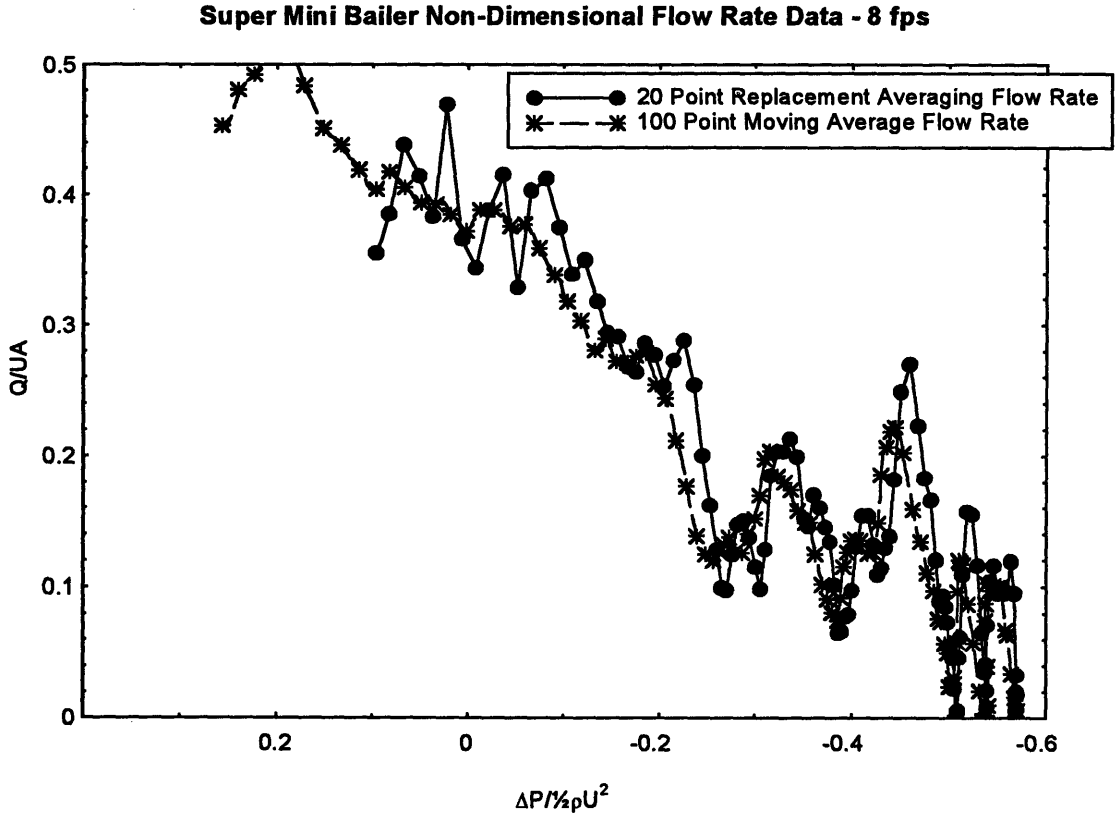

Figure 6.3 - Flow Rate Derivative Averaging Comparison

In order to appropriately characterize the performance of a bailer it is important to realize the actual application of the bailer and the likely conditions to be encountered. Examination of the pressure trace in Figure 6.2 shows that the pressure in the reservoir was in excess of 3500 Pa or 0.36 meters of positive hydrostatic pressure head above the

pressure acting externally on the bailer. In the case of actual operation this magnitude of head would exceed the available hull depth of a 470 class sailboat and would imply a serious flooding of both Star and Soling yachts. Clearly this is an unreasonable condition to consider in evaluating the relative merits of each bailer prototype. Perhaps the most interesting region of bailer flow rate occurs when the flow is solely drawn out as a result of the low pressure created behind the deployed bailer, without the effects of hydrostatic pressure in excess of the external pressure acting on the bailer. This region, depicted in Figure 6.2 after the intersection of the reservoir and tunnel pressure traces (or zero pressure difference point), can be used to quantify the ability of a particular bailer to generate suction, while the point at which flow rate ceases can be used to determine the speed of bailing inception as outlined previously. Hydrodynamically, the region beyond the zero pressure difference is of the most interest, but in actual application it is likely that bilge water levels above the yacht's water line may occur producing a hydrostatic pressure contributing to the outflow. To model this, a positive pressure of 300 Pa (corresponding to 3.06 cm) above the point of zero pressure difference was selected as a reasonable value for a yacht traveling at 8 feet per second. The data used for the comparison of bailers was extracted from the obtained experimental data for reservoir pressures lying between a point 300 Pa above the zero pressure difference point to the point of zero flow rate or equilibrium. To obtain corresponding pressure intervals for bailer experiments at higher speeds the 300 Pa interval was scaled by the square of the ratio of free stream velocities to produce equivalent starting points for each of the higher speeds. Accordingly, start points of 468.75 Pa and 675 Pa above the zero pressure difference point were selected for the 10 and 12 feet per second tests respectively.

Tests for each bailer were repeated to ensure that the data obtained correctly reflected reservoir starting pressures and conformed to the expected trends as depicted in Figure 6.2. It was noted that in humid testing conditions or in the event that sensor contacts were splashed very unreliable data was obtained. Similarly, over the entire period of testing it was noted that drifting of the pressure transducer signals occurred. While some of this can be attributed to the sensor warm up times which were allowed for prior to testing, the age of the transducers must also be considered as a factor, particularly in light of the poor results obtained in later tests.

Provided the critical assumptions regarding the non-dimensionalization of the critical parameters are correct, it is expected that for a given bailer the results from each of the three tested speeds should collapse into a single curve once they have been non-dimensionalized. Consideration of Figure 6.4 clearly shows the large degree of scatter between the three test speeds and the great discrepancy between the observed equilibrium pressure reading (as indicated by the vertical line) and that recorded by the pressure sensors. If these discrepancies are attributable to the drift in the pressure sensors and this change is assumed to affect the recorded traces by a constant amount we can correct each of the traces accordingly. An equilibrium pressure error was established as the difference between the equilibrium pressure recorded visually using the manometers and the value obtained from the pressure transducer measurements. These error values were then used to translate each of the pressure traces along the pressure axes such that the final equilibrium pressure indicated by the pressure traces corresponds to that measured visually from the manometers. Figure 6.5 represents the above correction applied to the data set

of Figure 6.4 and produces a noticeable reduction in the scatter of the data points. Once corrected the three curves largely collapse to a single curve decreasing until the equilibrium pressure is reached. Identical corrections were applied to the pressure data for each bailer to allow for comparison.

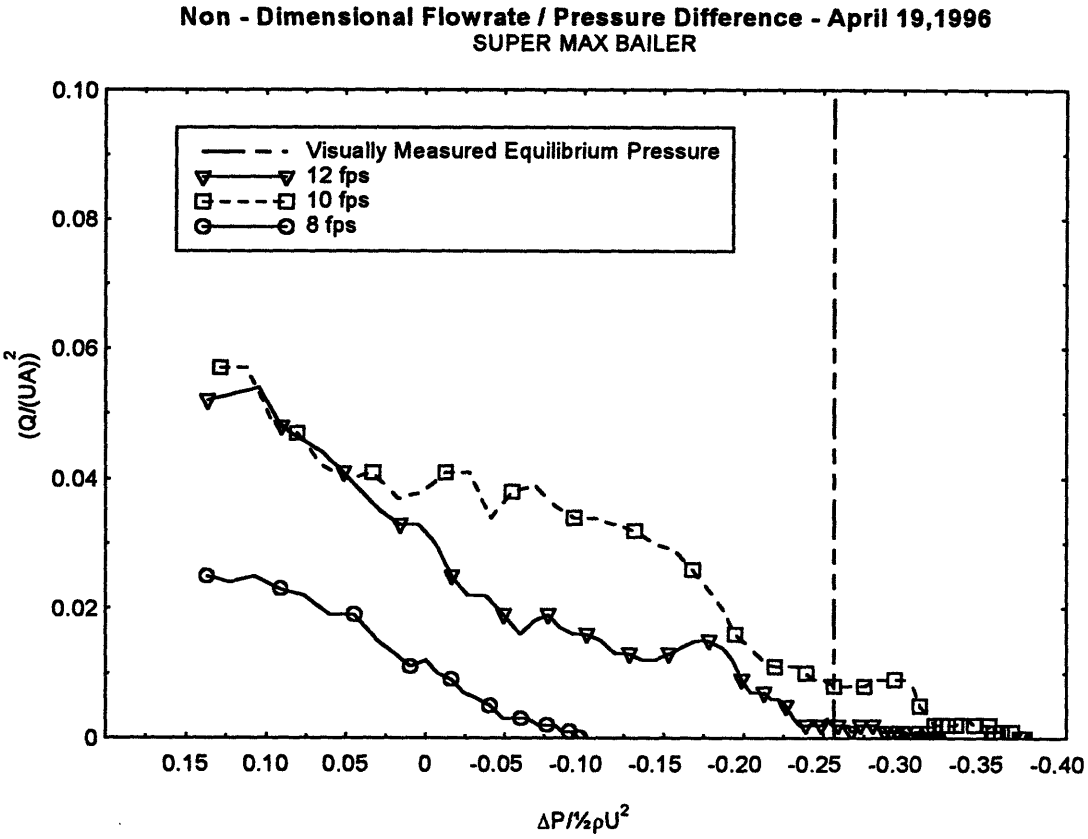

Figure 6.4 - Uncorrected Flow Rate Data

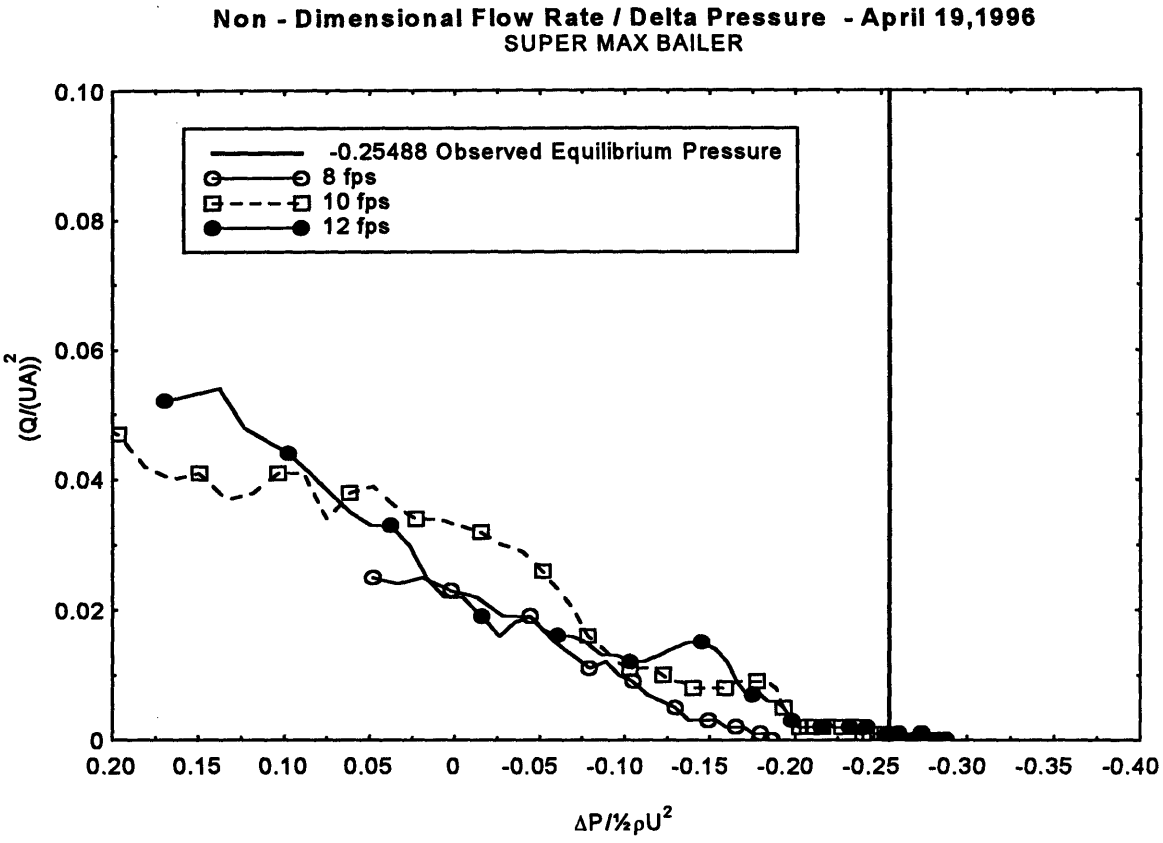

Figure 6.5 - Corrected Flow Rate Data

6.2 - Production Bailer Results

Figure 6.6, below shows the processed results of a series of tests at the three test speeds of 8, 10 and 12 feet per second. Super Mini experiments were repeated three times in order to establish baseline performance characteristics and the tests with the best correlation selected. A linear least squares fit to the data was also completed in order to confirm or dispel the expected linear relation between the square of the non-dimensional flow rate and the non-dimensional pressure difference over the course of the run.

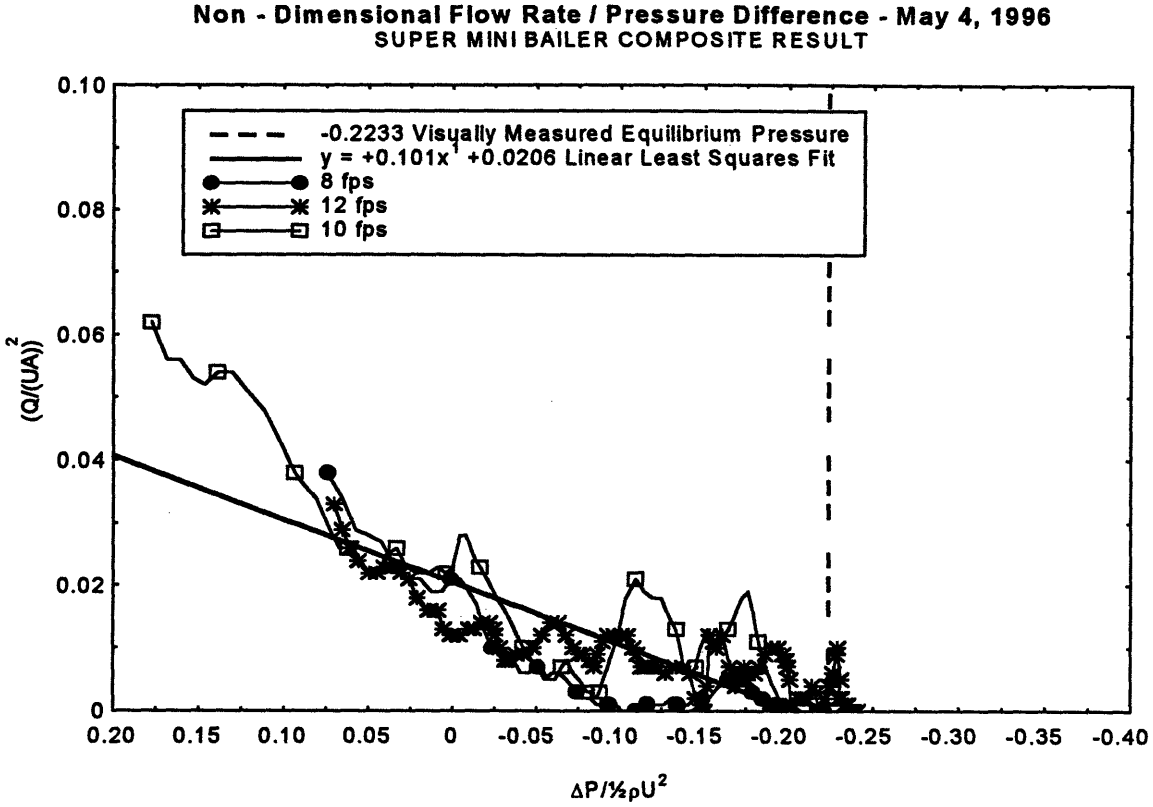

Figure 6.6 - Super Mini Bailer Non-Dimensional Flow Rate Results

Although the three traces collapse well to form a single trace, it is apparent that the linear least squares fit of the data which should bear out the derivation of Section 2.5 is somewhat deficient in defining the flow rate. This may be attributable to non-linear effects not accounted for in the derivation or more likely is a reflection of the difficulties in obtaining an adequately smoothed data set on which to perform the numerical differentiation. This is borne out subsequently in the flow rate plots for the other production bailers all of which exhibit some scatter.

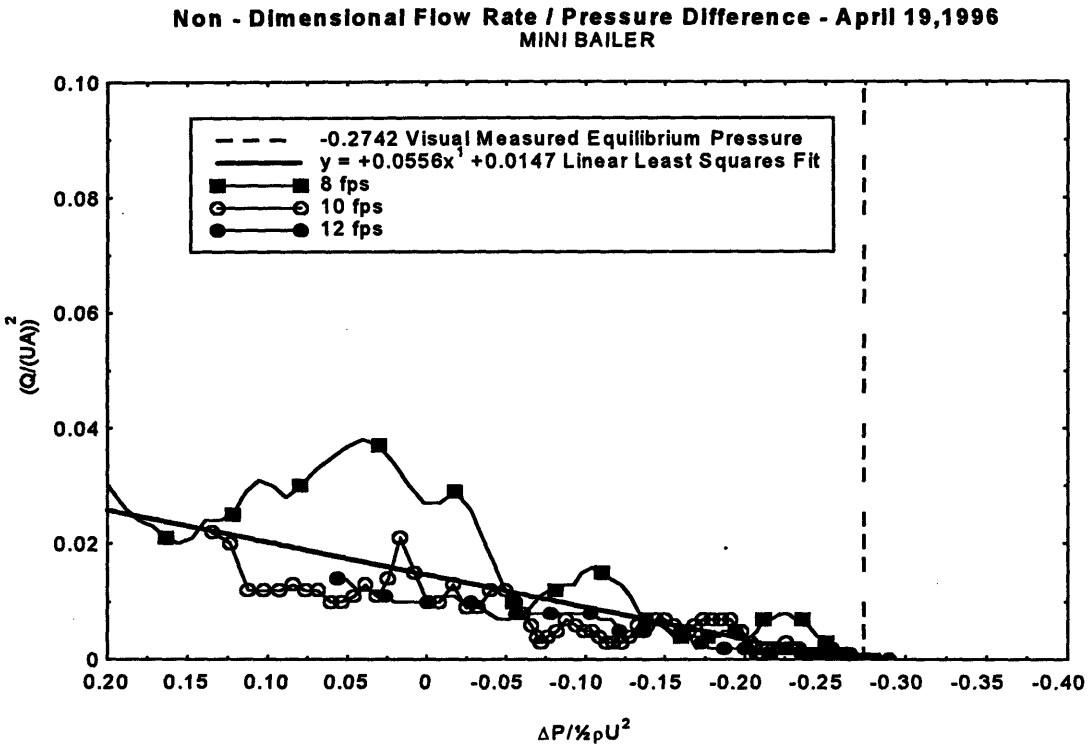

Figure 6.7 - Mini Bailer Non-Dimensional Flow Rate Results

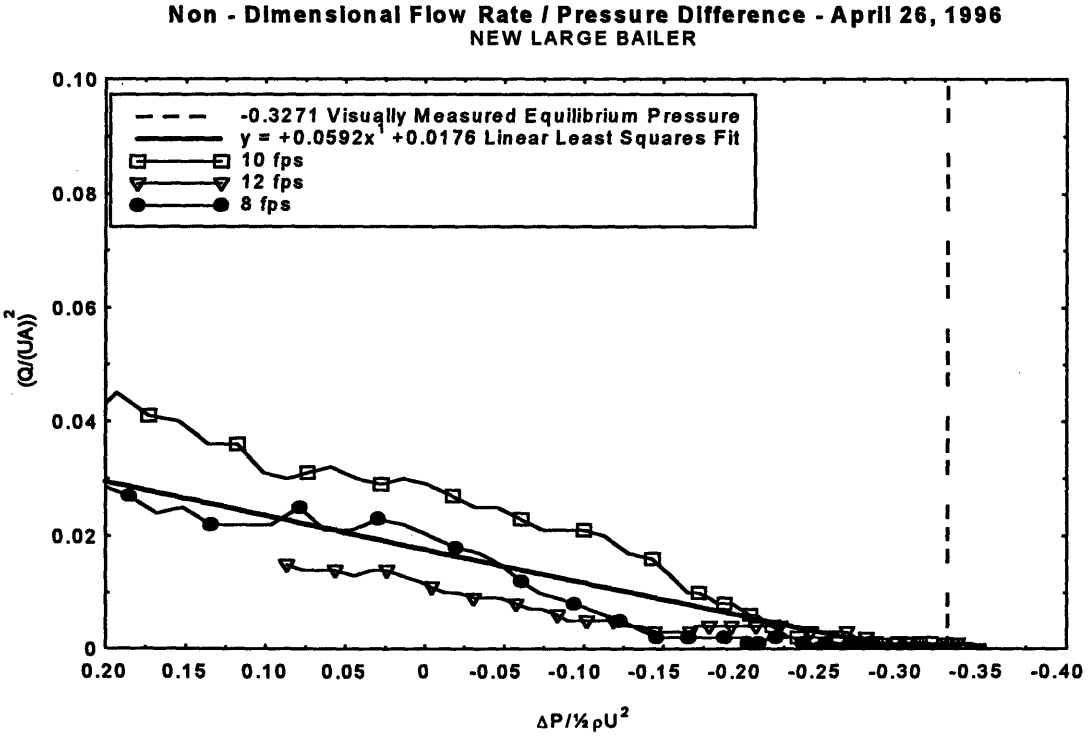

Figure 6.8 - New Large Bailer Non-Dimensional Flow Rate Results

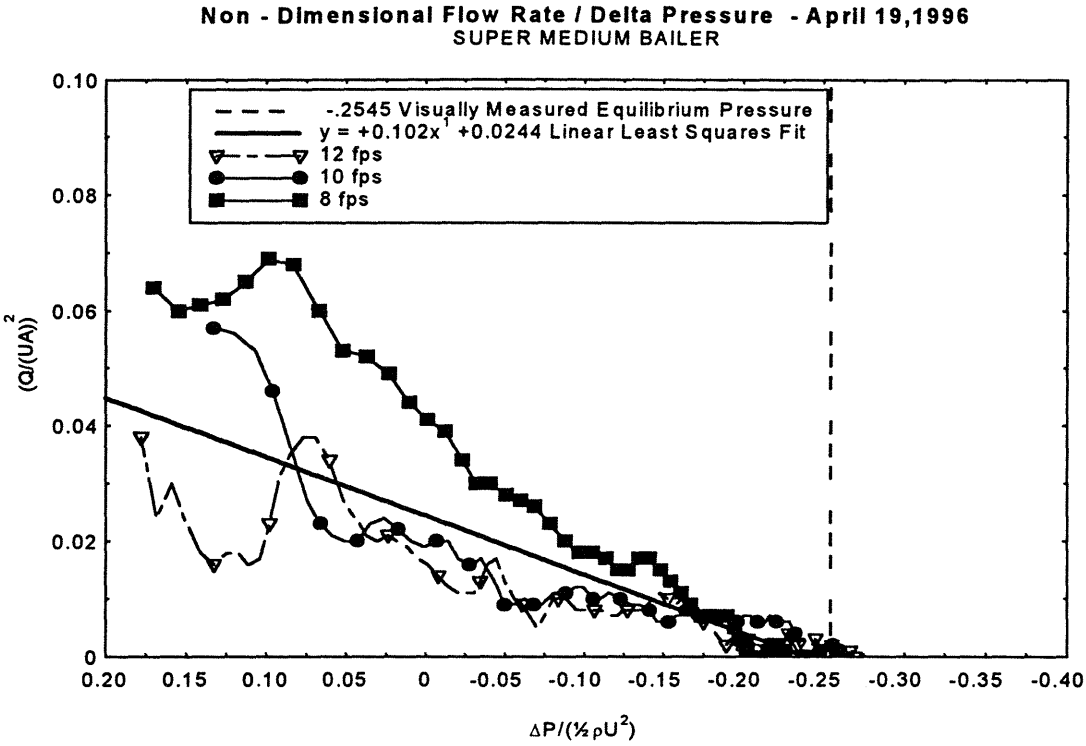

Figure 6.9 - Super Medium Bailer Non-Dimensional Flow Rate Results

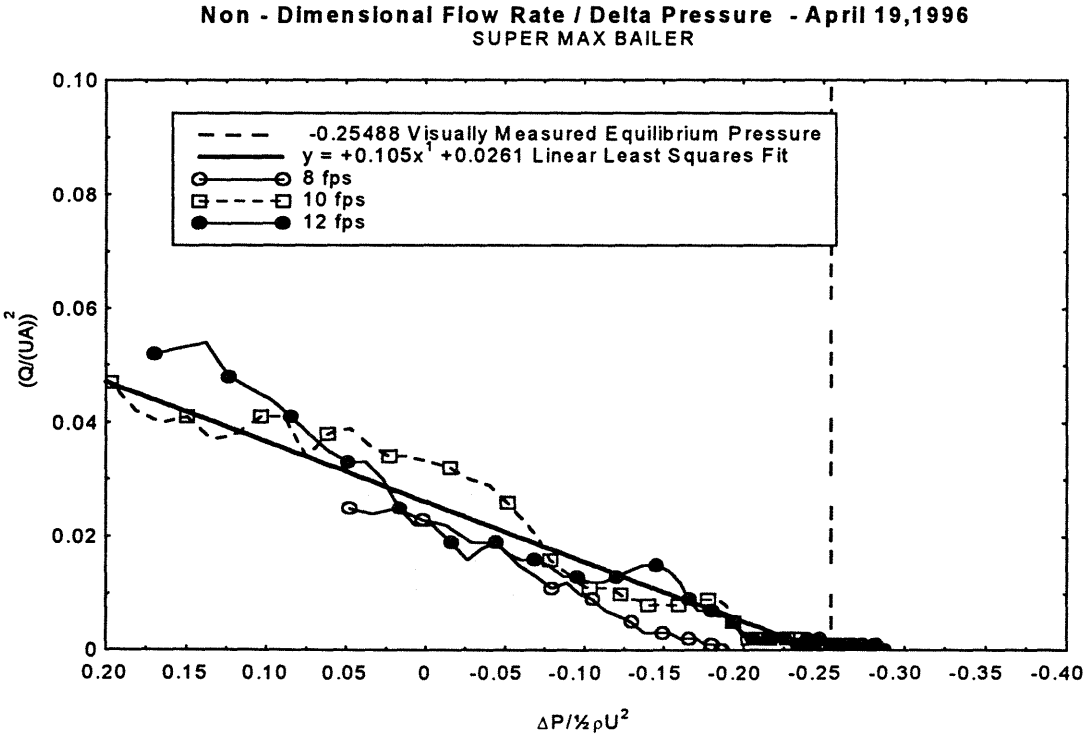

Figure 6.10 - Super Max Bailer Non-Dimensional Flow Rate Results

The preceding figures utilize a least squares linear curve fit to characterize the non-dimensional flow rate performance of each bailer. By comparing these linear curve fits it should be possible to compare the performance of each bailer and relate this to their geometric characteristics. The large degree of scatter present in each of the above data sets clearly indicates the possibility that the linear least squares curve fit may not correctly reflect the actual flow rate of a particular bailer making it difficult, if not impossible to compare the merits of different bailers. Indeed, the low correlation coefficients represented in many of the above data sets serves to emphasize this point and further questions the validity of the derived linear relationship between the square of the non-dimensional flow rate and the non-dimensional pressure difference across the bailer.

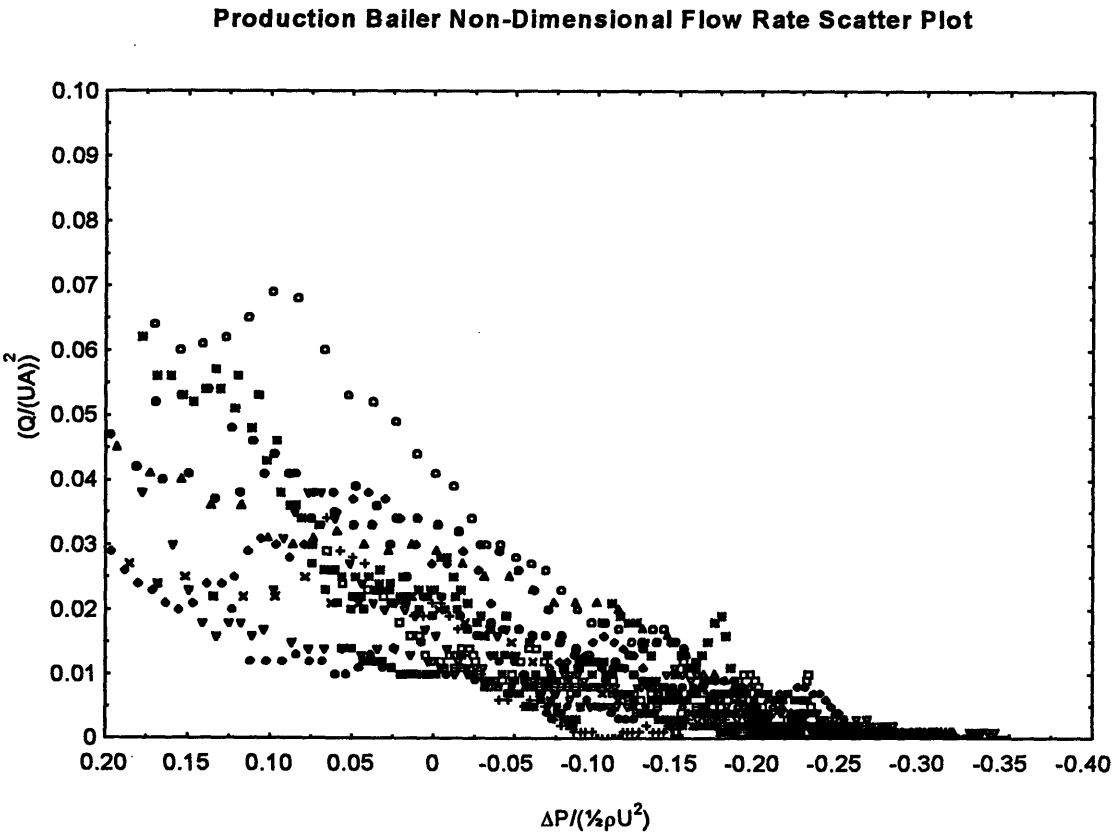

Figure 6.11 - Production Bailer Non Dimensional Flow Rate Scatter Plot

Figure 6.11 superimposes the results from all production bailer tests in non-dimensional form. Qualitatively, Figure 6.11 serves to illustrate the extent of the scatter and the observation that all flow rates decrease monotonically to the point of zero flow rate as expected. The extent to which this is a linear relationship cannot be determined from this figure, but it does serve to emphasize that, once non-dimensionalized, the relative performance of the bailers is similar.

6.3 - New Prototype Results

Although designed to capitalize on beneficial pressure distributions and low drag configurations, the flow rate results of both the Hydrofoil and Blister bailers are disappointing. As can be seen from Figure 6.12 below, the hydrofoil's performance in a non-dimensional sense, was below even the worst flow rates measured for any of the production bailers, with the Blister bailer achieving only on the order of 50% of the non-dimensional flow rate measured for the Hydrofoil.

A case must be made for the fact that the pressure suction drag governing the operation of the production bailers is utilized to a less extent in the Blister bailer and the hydrofoil bailer. For consistent non-dimensionalization the maximum sectional area of the blister and foil were used in calculating the non-dimensional flow rate. These projected areas are on the order of 50 to 100% larger than those measured for the production bailers and it is therefore expected that any non dimensional flow rates for the prototype bailers be smaller than that determined for the production bailers and their variations.

Even with these considerations, the actual geometry of the foil and the Blister severely limit their applicability to Olympic yachts. Almost all racing classes governed by a design rule have limitations on appendage sizes because of their effect on stability and windward performance. It can therefore be expected that the Hydrofoil bailer would be considered as an appendage when deployed possibly putting the yacht in breach of the class measurement rules.

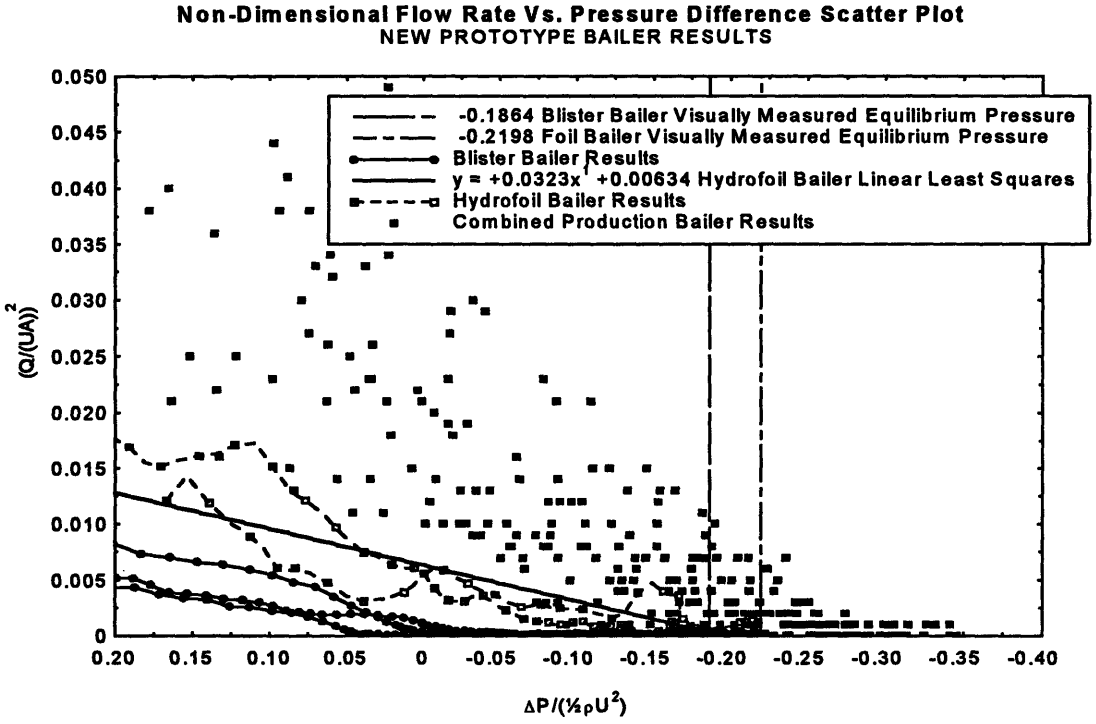

Figure 6.12 - New Prototype Non-Dimensional Flow Rate Results

Similarly, the Blister bailer's flow rate performance alone is reason to eliminate it from contention as a bailer, however, even if an acceptable flow rate could be achieved it would be difficult to design and construct a successful means of retraction.

6.4 - Modified Production Bailer Results

The most interesting results of the experimental program were observed in the testing of the modified production bailers. In particular, data from the Sideless Super Mini bailer indicates dramatic improvements over the production bailers in both flow rate and minimum speed of bailing inception.

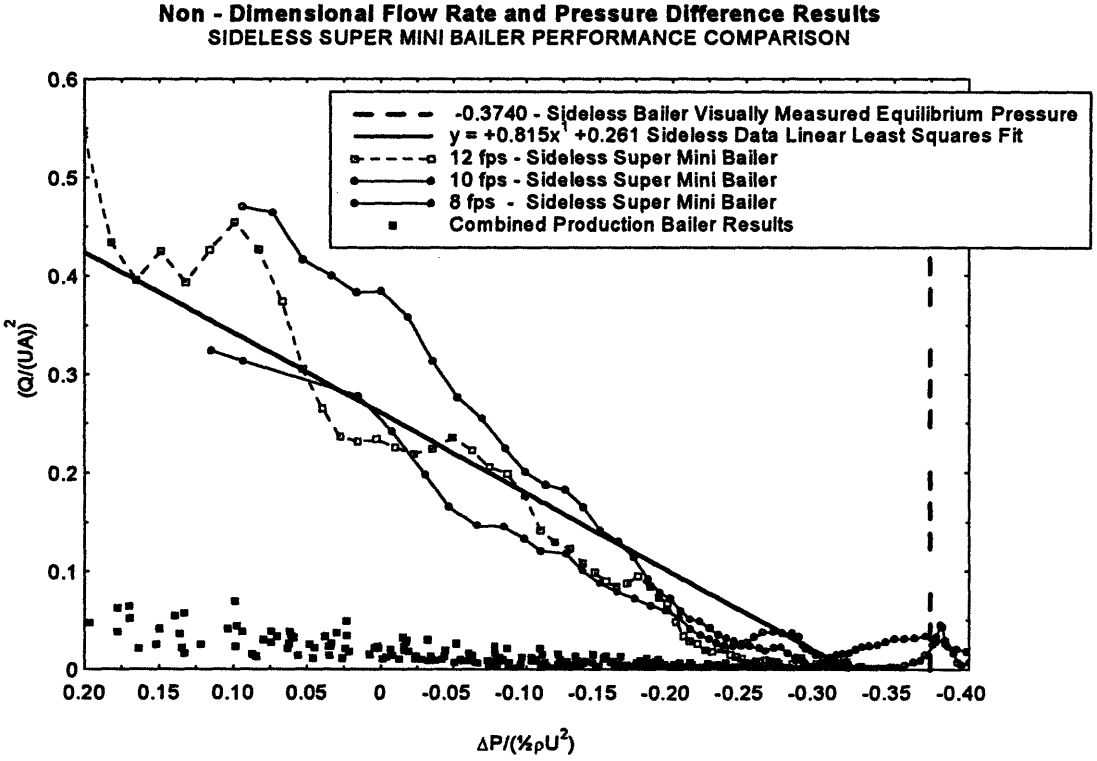

Figure 6.13 - Sideless Super Mini Bailer Non-Dimensional Flow Rate Results

Figure 6.13 represents the non-dimensional flow rate and equilibrium pressure points for the Sideless Super Mini bailer and the improvement shown is dramatic. Considering the achieved non-dimensional flow rate at the zero pressure difference position, the Sideless bailer achieves a flow rate more than three times greater than the best production bailer results. Production bailer data points are indicated by the scattered data at the lower

boundary of the figure. Also of considerable importance is the low pressure at the point of zero flow rate indicating that bailing inception will occur at a lower speed than any of the production bailers considered. Further discussion of bailer inception speed is considered in Section 6.5. As with the production bailer results it is apparent that a large degree of scatter is present in the data and that the linear least squares fit does not completely represent the trends in the data traces.

Although not as dramatic, the results from the testing of the Doorless Super Mini bailer also indicate an improvement over the production bailers. This serves to indicate that the limited size of the check valve door and thus the available outflow area, has a detrimental effect on the achievable flow rate of the bailer. While it stands to reason that a larger outflow hole will achieve a better flow rate, the reason for adopting an out flow hole of half the size of the available area is still uncertain. Strength considerations appear to be unlikely, but it is possible that the size of the outflow hole is limited by operability of the check valve door so that at low speeds only a small outflow is required to open the smaller door, whereas the larger door suggested by the experimental results may require a larger outflow for operation. No experiments were performed to investigate the effects on performance of larger check valve doors. Figure 6.14 below shows the performance of the doorless bailer in relation to the production bailers. Quantification of the magnitude of bailing improvement is again limited by the scatter of the data points, however, a conservative estimate of 75% to 150% improvement is indicated by the figure at the zero pressure difference point.

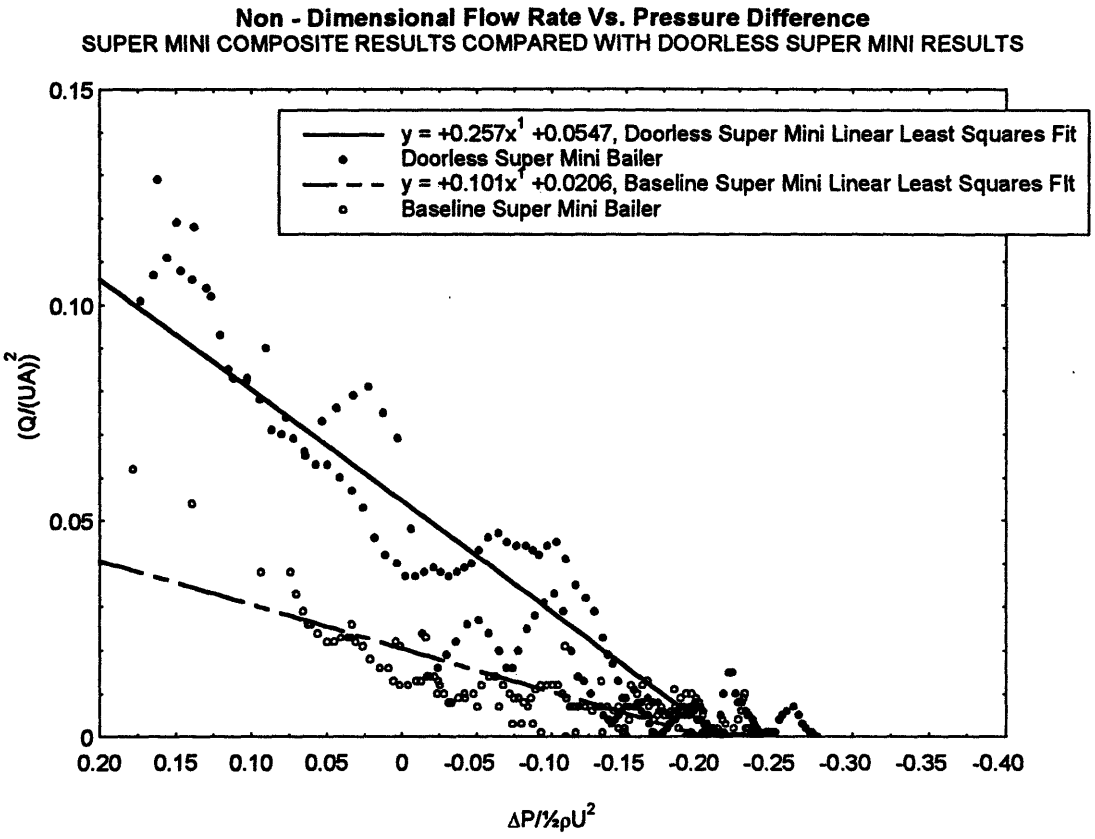

Figure 6.14 - Doorless Super Mini Non-Dimensional Flow Rate Results

As shown in Figure 5.7, one production bailer modification involved investigating the effects on flow rate of fairing the interior of a Super Medium Bailer. Such a modification will have no effect on the external hydrodynamics of the flow around the bailer and cannot contribute to the development of suction pressure. Nevertheless, any improvement in flow rate characteristics will be advantageous and can provide a simple means of improving the performance of a production bailer without altering the functionality of the current design.

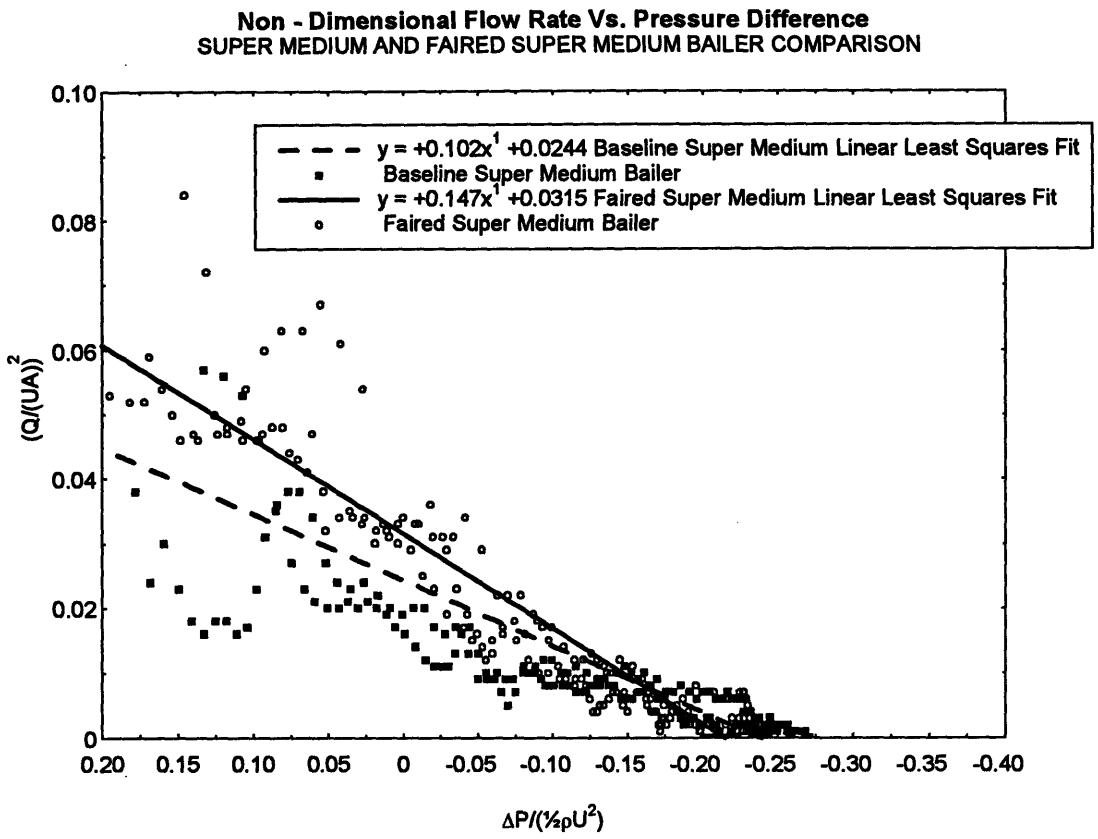

Figure 6.15 - Faired Super Medium Bailer Non-Dimensional Flow Rate Results

Despite the large data scatter present in Figure 6.15 above, it is suggested that over the majority of the pressure differences tested a faired inlet fitted to the Super Medium Bailer results in an improved flow rate over the comparable production bailer. The nature of the scatter diagram precludes an accurate quantification of the improvement although a conservative estimate of 10 to 15 % is indicated at the zero pressure difference point by comparison of the least squares fit lines. This result is as expected from the reduction in pressure losses in the bailer and the more uniform tangential flow through the outflow door. It can be expected that further modifications to improve the flow path into the bailer will produce significant improvements in bailer performance with no drag penalties whatsoever.

6.5 - Minimum Bailing Speed Results

As outlined in Chapter 3 the speed of bailing inception can be determined once the hydrostatic pressure between the bailer and an assumed waterline is known, and the equilibrium non-dimensional pressure difference is determined. To gain an estimate of the relative bailing inception speed performance of each configuration a head difference between bailer and waterline of 0.15 meters was assumed as a reasonable value for the Star and Soling classes and the bailing inception speed calculated. The table below represents these results:

Table 6.1 - Bailing Inception Speed Results

BAILER	C_p	Bailing Inception speed		
		m/s	ft/s	knots
Sideless Super Mini	-0.374	2.81	9.20	5.45
New Large	-0.327	3.00	9.84	5.83
Mini	-0.274	3.28	10.75	6.37
Super Max	-0.255	3.40	11.15	6.60
Faired Super Medium	-0.255	3.40	11.16	6.61
Super Medium	-0.255	3.40	11.16	6.61
Super Mini	-0.223	3.63	11.91	7.06
Doorless	-0.222	3.64	11.95	7.08
Foil	-0.220	3.66	12.01	7.11
Blister	-0.186	3.97	13.04	7.72

Table 6.1 contains a number of interesting results. The Sideless Super Mini and its variations clearly develop the minimum required suction pressure at speeds approximately one knot lower than the majority of the other production bailers except for the new large which has too much drag for small racing vessels. This is of great importance for

operation in lighter winds and during pre-start maneuvering. Also of particular note is the poor performance of the new prototype bailers. This is as expected considering the nature of the flow rate curves and indicates that the development of suction pressure is comparatively weak in the Hydrofoil and Blister bailers. In the case of the Super Medium Faired Inlet bailer the results indicate that this bailer will begin operation at the same speed as its production bailer cousin. This is expected as the fairing in no way modifies the external flow dynamics around the bailer and does not affect the development of the critical suction pressure.

Chapter 7 - Bailer Drag Test Results

7.1 - Drag Data Acquisition and Processing Methods

As outlined in Chapter 3 a separate experiment designed to minimize measurement and procedural errors was devised for determining bailer drag. This involved the testing of the bailer in the deployed condition but with the reservoir empty so that no outflow occurs. To improve confidence in the drag measurements every bailer, with the exception of the Super Max, was tested at least twice and drag values recorded at 6, 8, 10 and 12 feet per second. As a means of confirming the observed drag numbers, the 8 feet per second test was repeated at least twice for each bailer experiment. In a number of cases a speed of 14 feet per second was tested to attempt to gain a measure of the drag caused when ventilation occurs. Unfortunately, the turbulent nature of the air expulsion through the bailer caused oscillations in the recorded measurements and in most cases exceeded the dynamic range of the data acquisition board, preventing the acquisition of any useable data at this speed.

Each test of the closeable production bailers involved obtaining a zero reading, a tare reading with the bailer retracted and finally, the drag with the bailer deployed. The final reported drag number is the difference between the tare and bailing values and is converted into physical units by using the determined calibration constants for the particular experiment. As described previously, the drag value assigned to a particular bailer is the average of a sample of 12,000 data points from a minute's duration of measurement at the particular testing speed. Figure 7. below gives a clear indication of the degree of scatter in the drag measurements and supports the adoption of the average

value as the drag reading. Much of the oscillatory nature of the signal can be attributed to the apparatus design. This is particularly true of the movement of the reservoir apparatus within the window aperture, which presents a series of sharp edges that may enhance turbulence.

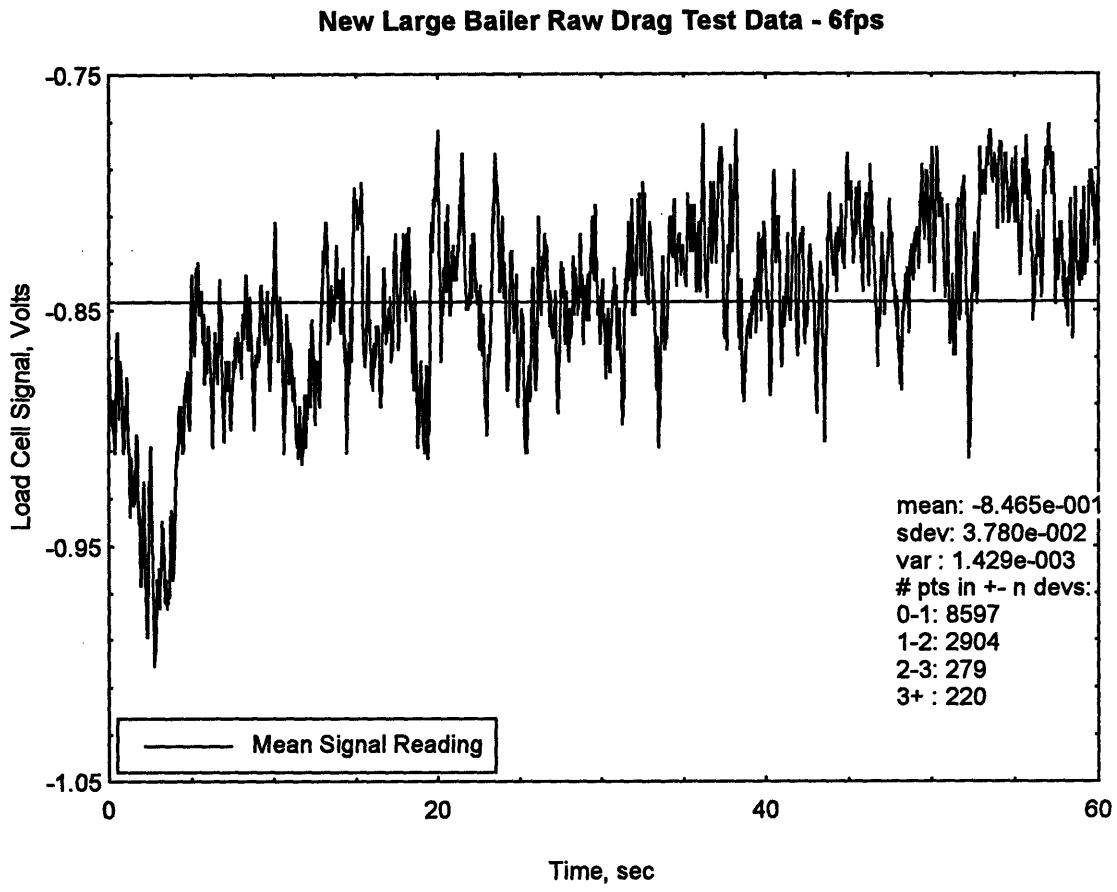

Figure 7.1 - New Large Bailer Raw Load Cell Signals

Furthermore, the nature of the tape positioned to fair incoming flow over the bailer appears to have affected the equalization of pressure around the aperture gap such that when speed was applied, the pressure differential between upstream and downstream regions in the aperture caused the entire apparatus to shift a measurable amount upstream

from the zero speed position. Equalization of this pressure difference may not be uniform and may occur at any time throughout the data acquisition run, contributing to the observed oscillations in the load cell signal.

For each series of tests drag area, defined as:

$$DragArea = \frac{Drag}{0.5\rho U^2} \qquad \text{Equation 7.1}$$

was calculated for each speed. After eliminating unreasonable values, the results were averaged to give a better representation of the drag area for a particular bailer. Further averaging of independent test series data for each bailer was then completed before calculation of the drag coefficient was performed as follows:

$$C_D = \frac{Drag}{0.5\rho U^2 A_{projected}} = \frac{DragArea}{A_{projected}} \qquad \text{Equation 7.2}$$

The drag coefficients were then used in an attempt to compare the relative drag characteristics of each bailer.

7.2 - Experimental Drag Results

A typical example of the drag results for a production bailer is shown below and clearly indicates a number of inconsistencies in the data. It is expected that the drag on the bailer should increase with the square of the speed and it is clear that this does not occur in the data shown below, particularly at the higher speeds. Also apparent is the wide variance in the data at the lower speeds, a phenomenon that can be partially explained by the inflooding of water into the reservoir through the check valve, causing an increase in the drag error discussed previously. At the higher speeds this effect is smaller because of the lower suction pressures at these speeds.

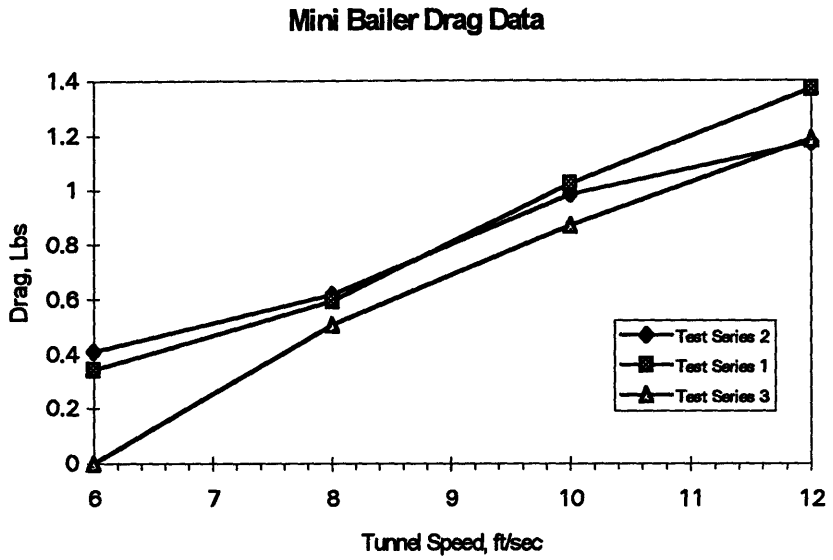

Figure 7.1 - Mini Bailer Drag Results

Figure 7.2 indicates the limited repeatability of the drag experiments over three separate trials. Similar results were obtained for both production bailers, the new prototypes and the production bailer variations and indicate a large amount of uncertainty in the results.

The following table displays the averaged drag areas for each bailer tested along with the drag coefficient calculated using the projected area of the bailer as the required length scale.

Table 7.1 - Averaged Drag Experiment Results

Bailer	Drag/½ρU², m²	Projected Area, m²	Channel/Face Width Ratio	C_D
Super Mini	0.000338	0.000684	0.760	0.49
Mini	0.000925	0.001155	0.528	0.80
New Large	0.001241	0.001872	0.641	0.66
Super Max	0.000648	0.001464	0.888	0.44
Super Medium	0.000624	0.001077	0.808	0.58
Sideless Super Mini	0.000443	0.000684	1.000	0.65
Blister	0.001364	0.004300	1.000	0.32

Of particular concern regarding the reliability of the data is the lack of correlation between the projected area, the channel to face width ratio, and the size of the drag coefficient. The magnitude of the pressure drag generated by the bailer is directly proportional to the size of the projected area and the base pressure generated by the bailer. Should the base pressures be identical between bailers the drag coefficients determined using the projected area would be equal. The data below shows that this is not the case and this scatter can be attributed to variations in base pressure between the bailers.

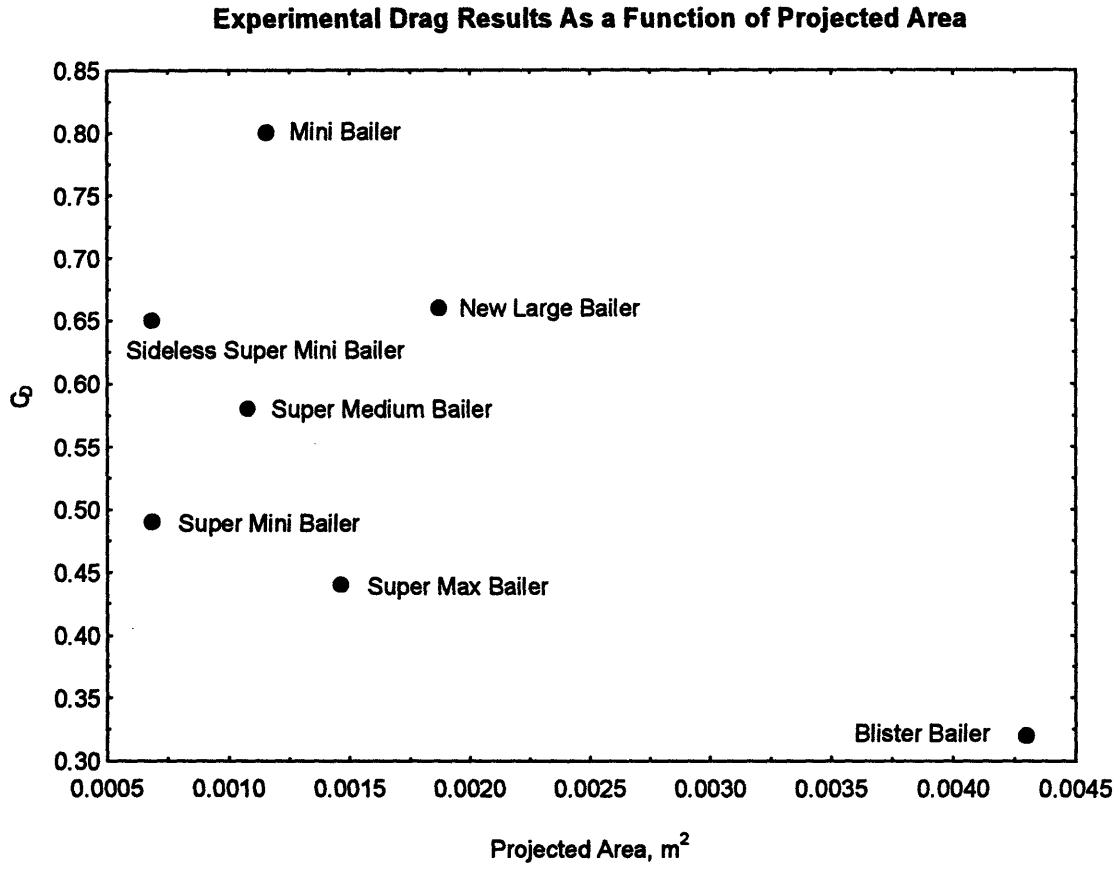

Figure 7.2 - Experimental Drag Results

The effect on drag of the channel to flange width ratio is also of particular interest particularly in the design of an optimum bailer. Figure 7.4 below indicates that, for the majority of production bailers, the drag coefficient decreases almost linearly as channel to

face width ratio increases. The Sideless Super Mini bailer has a 30 percent increase in drag coefficient over that measured for the baseline Super Mini bailer. A portion of this drag increase may be the result of added roughness due to the welding of the bailer into the open position and the fact that the tare measurements used in analyzing these drag results were adopted from a previous set of experiments. Even when corrected for the respective zeroes of each test it is expected that some experimental error remains between the tare and drag readings.

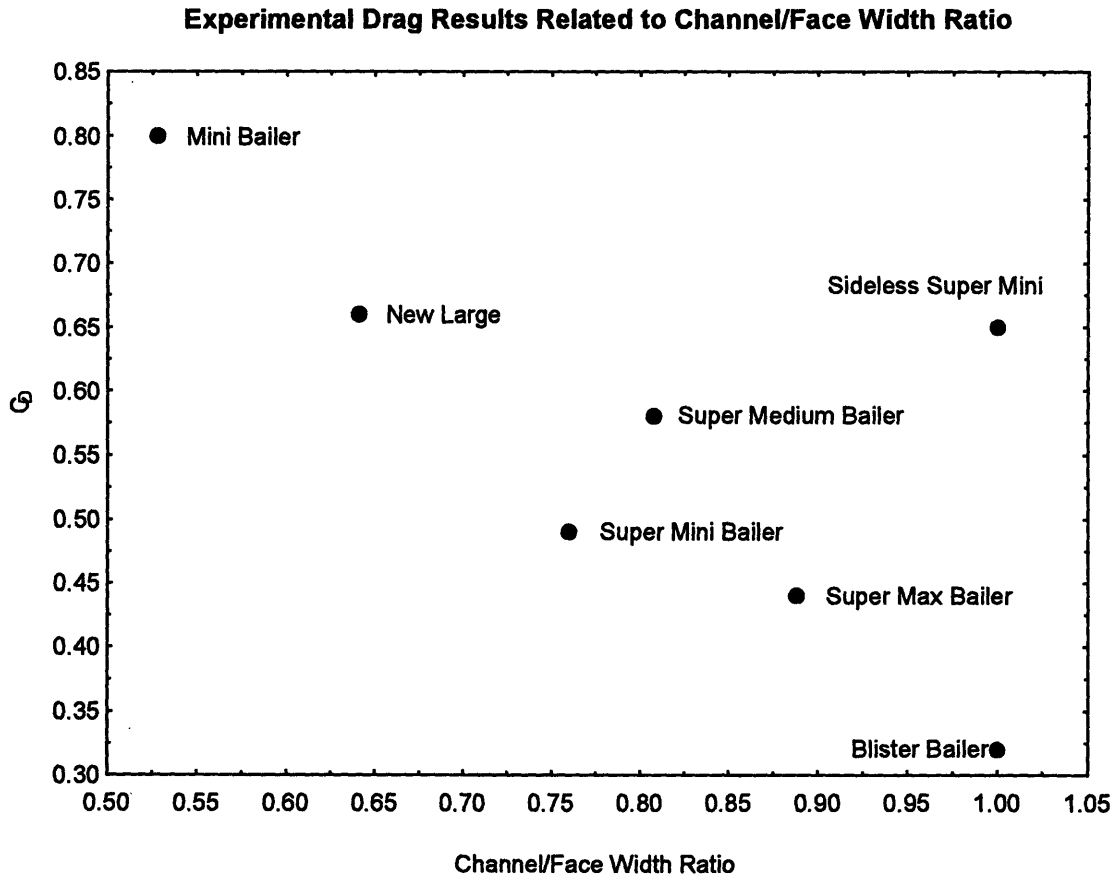

Figure 7.3 - Drag Coefficient Vs. Channel to Face Width Ratio

It should be noted that, if the sideless bailer does have a 30 percent drag increase, its drag would be made equal to that of the baseline Super Mini bailer by a 14 percent decrease in

dimensions. If this were done, its flow rate and bailing inception speed performance would still exceed that of the Super Mini by a large amount.

After consideration of the potential difficulties with the Hydrofoil bailer in regard to class rules, the poor flow rate data and the measurement difficulties presented in testing a bailer of such large size, no drag tests were completed for this bailer. Testing of the Blister bailer was completed in an effort to confirm that a low drag shape had been developed and to try and establish the extent of separation over the maximum extremity of the bailer. This bailer was tested in the closed position such that a fair body was presented to the flow as designed for the non-bailing condition. Because of the nature of the moveable forward section of the bailer, difficulties in sealing the seam between this section and the bailer installation plate allowed water to flood into the reservoir at the lower speeds contributing to the drag error described previously. Table 7.1 illustrates that the Blister bailer's faired form has a lower drag coefficient than any of the other bailers considered. However, like the Sideless bailer, the quoted drag measurement incorporates the use of a separately determined flat plate tare drag, possibly resulting in a considerable error.

Chapter 8 - Optimal Bailer Selection and Hydrodynamic Considerations

8.1 - Selection of an Optimum Design

While the drag experiment results fail to clearly isolate the relation between bailer geometry and the drag experienced, the order of magnitudes of the drag readings are all within the expected range. Similarly, the flow rate results could not adequately characterize the relative merits of the individual bailer geometry's with one exception; the Sideless Super Mini Bailer.

As is clearly depicted in Chapter 6, the Sideless bailer achieves on the order of three times the flow rate of even the best production bailer results at the point of zero pressure difference. The reason for this considerable advance in flow rate is dealt with subsequently, but its importance in defining a bailer with dramatically improved performance over the more traditional production bailers is indisputable. Consideration of the minimum bailing speed results also support this conclusion and the indicated improvements in the case of the Sideless bailer suggest that the bailer will operate at boat speeds up to one knot lower than the production bailers for the same application. The actual minimum bailing speed is dependent on the depth of bailer submersion below the yacht's waterline.

Examination of the Faired Super Medium bailer's performance in relation to the baseline Super Medium also suggests that improvements in flow rate can be achieved without modifications affecting the mechanical or hydrodynamic operation of the bailer. By simply fairing the inlet to the bailer a reduction in losses occurs, improving the flow

rate of the bailer and representing a simple, but important design feature to be incorporated in any future design.

8.2 - Sideless Super Mini Bailer - Governing Hydrodynamics

The obtained experimental results clearly indicate the superiority of the Sideless Super Mini bailer with regard to flow rate and bailing inception speed over the other bailers tested. While the determined drag coefficient is larger than some of the other bailers this may in part be due to the experimental and data processing difficulties outlined previously. The drag coefficient is 30% larger than that measured for the baseline Super Mini production bailer, however, the greater flow rate will dramatically reduce the amount of time the bailer needs to be deployed, considerably reducing the net amount of drag attributable to the bailer's operation over the course of a yacht race.

Section 2.5 outlined the generally held theory of the hydrodynamics governing the operation such bailing devices, however, this fails to adequately explain the dramatic improvements observed in flow rate and bailing inception speed as a result of removing the channel walls, check valve door and the remaining trailing face structure. The development of suction behind the face plate is a core component responsible for the magnitude of the flow rate, however, the achievable suction pressure must be of a similar magnitude to that produced by the intact production Super Mini bailer. This would necessarily limit the equilibrium pressure and as a result the bailing inception speed should be comparable for both bailers if this trailing face suction is the governing hydrodynamic phenomenon. The results clearly indicate that this is not the case and suggest that another phenomenon is contributing to the Sideless Super Mini bailer's

performance. While the Doorless Super Mini bailer achieved an improved flow rate over the base line it was considerably lower than that achieved by the Sideless bailer indicating that the improvement must directly involve the removal of the channel side walls.

To gain a visual understanding of the flow around the bailers, tests were completed at 14 feet per second causing all bailers to ventilate. In this way the entrained air could be used as a marker for the flow patterns around the bailer giving an insight into the phenomena at hand. All bailers of the Andersen - Elvstrom form (including the Sideless and Doorless variations) exhibited the development of large vortices from each of the exposed face plate edges. The trailing edge vorticity is integrally involved in the development of aft face pressure suction in all bailers but the side edge vortices present the most plausible explanation for the noted improvements in the Sideless bailer.

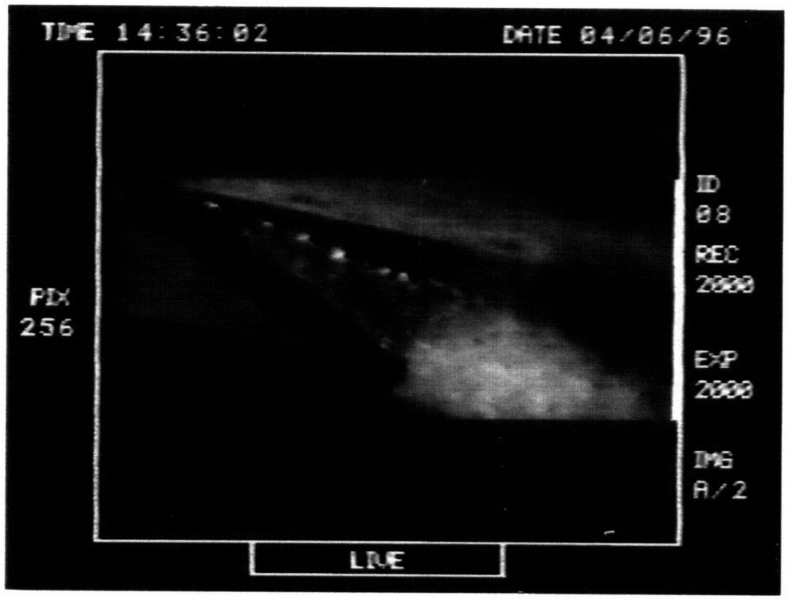

Figure 8.1 - High Speed Imaging of a Production Bailer Wake

Figure 8.1 contains a photograph of the wake generated from a ventilating production bailer in profile obtained using a high speed imaging camera. The turbulent nature of the wake immediately aft of the bailer is indicative of the suction pressure and the expulsion of air through the outflow door. Most importantly, the white line appearing in the foreground between the bailer housing and the face plate is the upper boundary of the trailing vortex that appears to be responsible for the improved performance of the Sideless bailer. The use of a similar photographic technique failed to adequately illustrate the development of the vortices on the Sideless bailer, largely due to the air being expelled from the sides of the bailer. Nevertheless, a visual examination of the Sideless bailer in the operating condition indicated vortices of considerably larger size than the baseline being shed from each side. In the vertical direction these vortices appear to impinge on the bailer mounting plate indicating a marked increase in vortex intensity over the production bailer depicted above. This increase in vortex size may be a physical manifestation of the phenomenon responsible for the larger drag coefficient determined for the Sideless Super Mini bailer. A diagram more clearly showing the action of these vortices on both Super Mini and Sideless Super Mini bailers is shown in Figure 8.2.

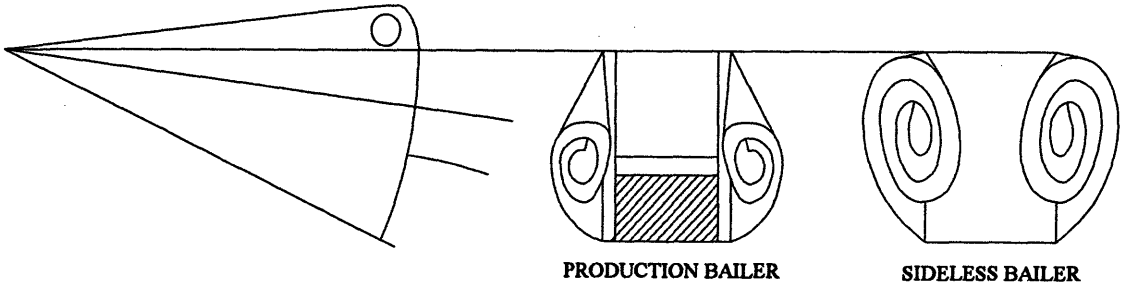

Figure 8.2 - Production and Sideless Bailer Wake Vortex System Comparison

The low pressure created at the center of these trailing vortices acts to draw the water (or air) out through the now open sides of the bailer improving the bailer's performance. In the production bailers these vortices impinge on the side walls of the channel and act only to increase the drag generated by the bailer with no contribution to flow rate performance. These vortices also provide a reason for the low bailing inception speed reported for the Sideless bailer. At lower speeds, the suction generated by the projected area of the bailer may be insufficient to cause outflow. However, the action of the vortices, which are present even at low speeds, may be sufficient to create the minimum required suction pressure.

8.3 - Other Design Considerations

The Sideless bailer as tested, was not in an operational form and acted as a prototype to investigate the effects of removing the channel walls and aft face structure. Having identified the dramatic improvements achievable through this design, further requirements must be met to produce an operable bailer.

Clearly, the optimum bailer design will take advantage of the shed vortices to dramatically improve flow rate and bailing inception speed performance. By fairing the inlet surfaces to the bailer, minimizing flow restrictions and encouraging tangential flow through the outlet further flow rate improvements can be made and such features should be incorporated in a proposed design.

Operability is of great importance in a bailer design and encompasses the ease of the mechanism's operation, its ability to repeatably withstand heavy - handed operation, and most importantly, the ability of the bailer to seal completely in the retracted condition.

In typical pre-race maneuvers it is common for the yachts to stop and in some cases drift in reverse. In all cases it is desirable to start a race with the driest boat possible and consequently, bailers are often left down during this maneuvering period. It is essential that a operational bailer have an automatic check valve mechanism to prevent a large inflow when insufficient speed is present to generate the required suction pressure. As outlined previously, the production bailers utilize a pin-hinged trap door located on the aft face of the bailer to act as check valve, minimizing inflow in those situations where insufficient speed is available.

The proposed design of a production Sideless bailer consists of a face plate hinged at the upstream edge, with a tongue extending into the boat. When this tongue is pressed down, the interior portion of the face plate locks down, retracting the bailer plate and maintaining enough force to completely seal the bailer plate into the recessed housing. When open, the available inflooding area is much larger than that of any of the production bailers and the use of a trap door mechanism is essential. The initial proposal for a trap door mechanism uses a door of smaller area than the face plate, hinged at the leading edge. When the bailer is operating the trap door will rest flush on the face plate and will not restrict outflow. In the case of back flow this trap door will pop up, sealing the bailer. Gravity will not help close the valve so it is suggested that the valve be made of a buoyant material such that the buoyancy will assist in closing the trap door. Preliminary tests of this idea indicate that it will close and seal the opening, however, a small delay in the closing of the valve occurs before the inflow catches the underside of the valve forcing it up. To improve the response time of the valve it is suggested that the check valve door be made

dished at the downstream end or with a small tapered rib underneath such that any inflow will more efficiently operate the valve. These problems with the valve door can be attributed to the action of the trailing vortices which may act to hold the door down as speed drops and bailing ceases. Figure 8.3 depicts the proposed Sideless bailer design and the different check valve door formations.

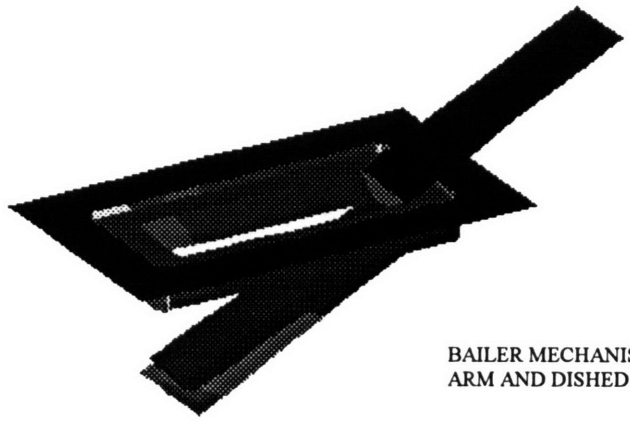

BAILER MECHANISM WITH OPERATING ARM AND DISHED PLATE CHECK VALVE

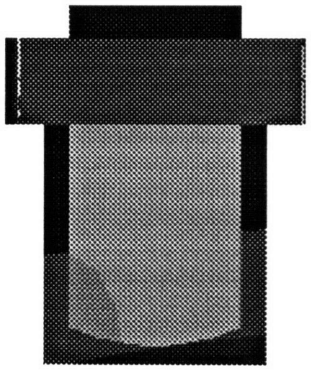

DISHED PLATE CHECK VALVE

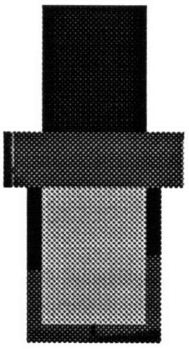

RIBBED PLATE CHECK VALVE

Figure 8.3 - Proposed High Performance Bailer Design Including Check Valve Mechanisms

An alternate check valve mechanism was developed by Mr. Arnold Heitmann utilizing a mechanism interior to the boat and an operating rod affixed to the face plate. This configuration is depicted in Figure 8.4 and consists of a tubular cover affixed above the face plate housing. This cover is open at the bailer's up stream end so as to allow the water to flow into the mechanism and a hinged door is located within the housing to act as a check valve and to prevent inflow when speed is below the minimum required for operation.

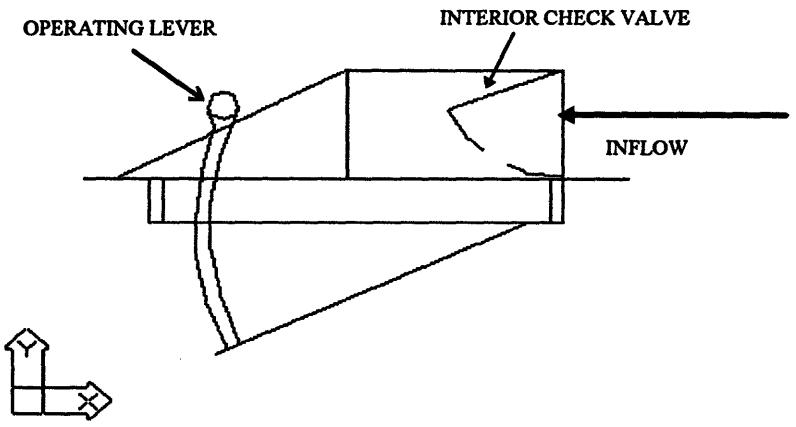

Figure 8.4 - Heitmann Check Valve Mechanism

Preliminary results indicate the performance is comparable to the Sideless prototype. The fairing will restrict the flow of water into the bailer while operating. Should the water level drop below the inlet orifice it is questionable as to whether the water will have enough momentum to hold the check valve door open to allow for outflow. Also, the use of the operating rod to deploy and retract the bailer may present some difficulties both in sealing the region between the rod and its opening in the bailer fairing, and structurally in it's ability to withstand heavy handed operation by the crew.

Chapter 9 - Conclusions

9.1 - Summary

A successful experiment has been developed to investigate the relative performance of sailboat self bailing devices and has provided a greater understanding of the hydrodynamics governing the operation of these devices. By systematically modifying the geometry of the production bailers it has been possible to develop a bailer that better takes advantage of the actual hydrodynamics of the flow, particularly the use of the wake vortices in creating low pressure regions that dramatically improve flow rate and minimum bailing speed performance. In the "traditional" production bailer design these vortices contribute to the drag force on the bailer and are utilized only slightly at best to improve either flow rate or bailing inception speed performance.

While the experiment has determined the considerable performance improvements available by removing the channel side plates and aft structure, the resolution of the experiment was not adequate to capture the relative effects of the various production bailer geometries on flow rate and bailing inception speed performance. This is in part attributable to difficulties in the data related to drifting in the pressure transducers and unsteadiness in the tunnel pressure.

The use of low drag forms with favorable pressure distributions was investigated by the construction of two prototype bailers. These bailers clearly produced the lowest flow rates and the worst bailing speeds of any of the tested bailers. However, these drag coefficients were demonstratively lower than those determined for the other bailers. This

is in part due to the large projected area of these prototypes which is inversely proportional to the calculated drag coefficient. From this result it is apparent that there is a definite coupling between the hydrodynamic phenomena contributing to drag and those contributing to the flow rate and bailing inception speed performance.

The obtained drag results exhibit a great deal of variance, and it is not felt that these results can adequately be used to compare the drag performance of the individual bailers and their respective geometries. Much of this error can be attributed to experimental difficulties directly related to the apparatus and the measurement of drag within a very turbulent and unsteady flow.

Despite the difficulties in drag measurements, the superior flow rate and bailing inception speed performance of the Sideless Super Mini bailer illustrates the importance of a systematic study of bailer geometries. If the features of this bailer are incorporated into a production design that successfully meets a number of operabilty requirements then the required bailer operation time to remove the same amount of water as a traditional bailer will be considerably reduced. Provided the bailer is only deployed for the minimum required time, the net drag increase on the yacht as a result of the bailer over the course of a race will be considerably reduced, directly translating into a competitive advantage.

9.2 - Recommendations for Future Work

The experiment utilized in determining the performance of each bailer could be improved by utilizing more sensitive pressure sensors that are better isolated to the external environment, eliminating humidity and dampness effects on the sensors. Furthermore, an accurate mounting of the reservoir apparatus within the window such that

the compression rods are accurately mounted in their vertical orientation such that the change in position of the center of gravity of the water as it is expelled will not create a moment inducing an apparent drag reading. If this can be successfully completed coupled measurements of both flow rate and drag would be attainable giving a better representation of the drag characteristics of the bailer over the course of its operation. Testing of operational prototypes that are retractable would eliminate a great deal of the error associated with the tare (flat plate) drag measurements.

Operationally, further work should be completed to investigate remote operating mechanisms for the bailer and to confirm that the suggested check valve designs operate successfully.

Improved testing of the bailer's drag characteristics in the deployed but non-operating mode, may be achieved by fully submerging the bailer in the center of the tunnel on a mounting plate. Provided an appropriate boundary layer thickness is stimulated the Laser Doppler Velocimeter could be used to map the velocity profiles at a control volume's boundary and the drag on the bailer calculated. Similarly, numerical simulation of the flow around the bailer may be possible, however, the problem is complicated by the geometry and the fact that almost all hydrodynamic phenomena occur within a turbulent boundary layer.

Finally, it is interesting to consider the effect of both increased displacement due to shipped water on resistance and the resistance contribution made by the bailer. A velocity prediction program (VPP) model can be generated for the considered boats and a study of

the effects of increased displacement on the boat's resistance and race performance completed.

References

[1] Abbott, I. H., Von Doenhoff, A.E., *Theory of Wing Sections,* Dover Publications Inc., New York, 1959.

[2] Kerwin, J.E., et al., "An Experimental Study of a Series of Flapped Rudders.", *J. Ship Res.*, Vol. 16., 4, pg 225, 1972.

[3] Newman, J.N., *Marine Hydrodynamics*, The MIT Press, Cambridge, Massachusetts, 1977.